



## OPEN ACCESS

## EDITED BY

Davide Tiranti,  
Agenzia Regionale per la Protezione  
Ambientale del Piemonte (Arpa  
Piemonte), Italy

## REVIEWED BY

Michele Freppaz,  
University of Turin, Italy  
Alexandru Onaca,  
West University of Timișoara, Romania

## \*CORRESPONDENCE

Stefan Haselberger,  
✉ stefan.haselberger@univie.ac.at

RECEIVED 20 August 2023

ACCEPTED 02 October 2023

PUBLISHED 12 October 2023

## CITATION

Haselberger S, Scheper S, Otto J-C,  
Zangerl U, Ohler L-M, Junker RR and  
Kraushaar S (2023), Catchment-scale  
patterns of geomorphic activity and  
vegetation distribution in an alpine glacier  
foreland (Kaunertal Valley, Austria).  
*Front. Earth Sci.* 11:1280375.  
doi: 10.3389/feart.2023.1280375

## COPYRIGHT

© 2023 Haselberger, Scheper, Otto,  
Zangerl, Ohler, Junker and Kraushaar.  
This is an open-access article distributed  
under the terms of the [Creative  
Commons Attribution License \(CC BY\)](#).  
The use, distribution or reproduction in  
other forums is permitted, provided the  
original author(s) and the copyright  
owner(s) are credited and that the original  
publication in this journal is cited, in  
accordance with accepted academic  
practice. No use, distribution or  
reproduction is permitted which does not  
comply with these terms.

# Catchment-scale patterns of geomorphic activity and vegetation distribution in an alpine glacier foreland (Kaunertal Valley, Austria)

Stefan Haselberger<sup>1\*</sup>, Simon Scheper<sup>2,3</sup>, Jan-Christoph Otto<sup>4</sup>,  
Ulrich Zangerl<sup>1</sup>, Lisa-Maria Ohler<sup>4,5</sup>, Robert R. Junker<sup>4,5</sup> and  
Sabine Kraushaar<sup>1</sup>

<sup>1</sup>Department of Geography and Regional Research, University of Vienna, Vienna, Austria, <sup>2</sup>Dr. Simon Scheper—Research Consulting Teaching, Dähre, Germany, <sup>3</sup>Environmental Geosciences, University of Basel, Basel, Switzerland, <sup>4</sup>Department of Environment and Biodiversity, University of Salzburg, Salzburg, Austria, <sup>5</sup>Department of Biology, Evolutionary Ecology of Plants, University of Marburg, Marburg, Germany

The interaction between geomorphological and ecological processes plays a significant role in determining landscape patterns in glacier forelands. However, the spatial organization of this biogeomorphic mosaic remains unclear due to limited catchment-scale data. To address this gap, we used a multi-proxy analysis to map potential geomorphic activity related to surface changes induced by sediment transport on drift-mantled slopes and a glaciofluvial plain. High-resolution vegetation data were used to generate a catchment-scale map delineating vegetation cover and stability thresholds. The two maps were integrated, and an exploratory regression analysis was conducted to investigate the influence of geomorphic activity on vegetation colonization. The multi-proxy analysis resulted in an accurate mapping of catchment-wide geomorphic activity, with a validation accuracy ranging from 75.3% through field mapping to 85.9% through plot sampling. Through vegetation cover mapping, we identified biogeomorphic stability thresholds, revealing a mosaic of vegetation distribution. Distinct colonization patterns emerged across different geomorphic process groups, influenced by process magnitude and the time since the last disturbance event. The exploratory regression analysis showed that vegetation distribution is significantly affected by geomorphic processes. Based on the overlay of results regarding geomorphic activity and vegetation distribution, we suggest an age-independent framework that indicates four potential situations of biogeomorphic succession.

## KEYWORDS

biogeomorphology, proglacial, multi-proxy-analysis, vegetation distribution, geomorphic activity, catchment-scale, disturbance and stability

## Introduction

Understanding ecosystem development is crucial for its prediction and management (Larsen et al., 2020; Viles, 2020). Central to this development is the interplay between abiotic and biotic elements, as seen in the nexus between geomorphic activity and vegetation dynamics (Viles, 1988; Dietrich and Perron, 2006; Viles, 2020).

Glacier forelands display a spectrum of geomorphic processes and diverse stages of vegetation succession, underscoring their value as exemplary study sites for biogeomorphic investigation (Matthews, 1992; Klaar et al., 2015; Fickert, 2017; Fischer et al., 2019; Wojcik et al., 2021; Bosson et al., 2023). Terrain that is freshly exposed after deglaciation provides vast amounts of unconsolidated sediment, which is intensively reworked (Carrivick and Heckmann, 2017; Porter et al., 2019) during a transient phase termed paraglacial period (Ballantyne, 2002). Sediment reworking either stops when potential sediment sources are exhausted or sediments are stabilized through vegetation (Gurnell et al., 2000; Ballantyne, 2002; Curry et al., 2006). This process of stabilization is closely linked to soil formation, with the latter enhancing growth conditions for colonizing species while also being influenced by vegetation through the contribution of initial organic material by early colonizers (Burga et al., 2010; D'Amico et al., 2014; Wietrzyk et al., 2018). During primary succession, plants first colonize bare substrates, leading to a progressive increase in vegetation cover and a higher diversity in plant composition (Chapin et al., 1994; Fastie, 1995; Caccianiga et al., 2006; Junker et al., 2020). Allogenic factors, including geomorphic activity, substrate availability, water and nutrient supply and autogenic factors, including propagule presence and facilitative processes, create a diverse mosaic of successional stages (Matthews, 1992; Cutler et al., 2008b; Bormann and Likens, 2012; Erschbamer and Caccianiga, 2017). These stages manifest as vegetation patches with distinct sizes and compositions (Raffl et al., 2006; Marteinsdóttir et al., 2010).

Geomorphic activity is a potential disturbing factor for vegetation (Viles et al., 2008). The growth and spread of plants are limited by erosion and deposition processes through the destruction of biomass and by removing key resources (Matthews, 1999; Moreau et al., 2008), yet intermediate geomorphic activity can result in greater diversity (Connell, 1978; Huston and Huston, 1994; Richards et al., 2002; Sitzia et al., 2016). Conversely, denser vegetation cover mitigates geomorphic activity (Marston, 2010; Haselberger et al., 2021; Ohler et al., 2023). The leaf canopy intercepts rainfall, diminishing its kinetic energy, while the root systems secure the substrate (Isselin-Nondedeu and Bédécarrats, 2007; Graf et al., 2009; Haselberger et al., 2021).

The interaction of vegetation stabilizing sediment and geomorphic processes disturbing succession is conceptualized in the biogeomorphic succession model (Corenblit et al., 2009; Eichel et al., 2016). This model identifies stability thresholds represented by plant cover levels, wherein plants mitigate geomorphic process rates and stabilize terrain (Eichel et al., 2016; Haselberger et al., 2021; Ohler et al., 2023). Cover thresholds signal distinct phases of biogeomorphic succession (Haselberger et al., 2021; Eichel et al., 2023).

In high mountain environments, biogeomorphic studies have demonstrated the link between geomorphic activity and vegetation distribution at the plot scale, evident in landforms like solifluction lobes (Eichel et al., 2017), drift-mantled slopes (Eichel et al., 2016; Eichel et al., 2018; Haselberger et al., 2021) and alluvial fans (Lane et al., 2016). However, catchment-wide studies on this interplay are notably sparse (Renschler et al., 2007; Eichel et al., 2013; Klaar et al., 2015; Thoms et al., 2018), despite their importance for understanding long-term landscape evolution (Summerfield, 2005; Cutler, 2010; Reinhardt et al., 2010). The limited research

in this area can be attributed to the variability in geomorphic process intensities, challenges in obtaining comprehensive vegetation data for entire catchments, and the complexity of identifying appropriate proxies for geomorphic activity (Heckmann et al., 2016b; Fischer et al., 2019).

This study aims to derive information on catchment-wide geomorphic activity and vegetation distribution and assess how geomorphic processes affect vegetation colonization dynamics. The Kaunertal Valley in Tirol offers optimal conditions for this study, with its well-documented glacier retreat stages, ongoing paraglacial adjustment, and observable primary succession patterns. Based on the assumption that a combination of methods is better suited for detecting various geomorphic processes, we employed a multi-proxy-analysis to produce a catchment-scale map of geomorphic activity. Catchment wide vegetation cover is based on high-resolution unmanned aerial vehicle (UAV) data (Zangerl et al., 2022) and categorized based on stability thresholds obtained in previous studies (Haselberger et al., 2021). To examine the influence of geomorphic activity on vegetation distribution, we conducted an exploratory regression analysis that included information on abiotic site conditions. With this set of methods, we aim to answer the following research questions:

RQ1 To what extent does a multi-proxy analysis provide a reliable measure of geomorphic activity within a catchment-scale proglacial environment?.

RQ2 How do vegetation cover and stability thresholds change over time and vary among different geomorphic process groups?.

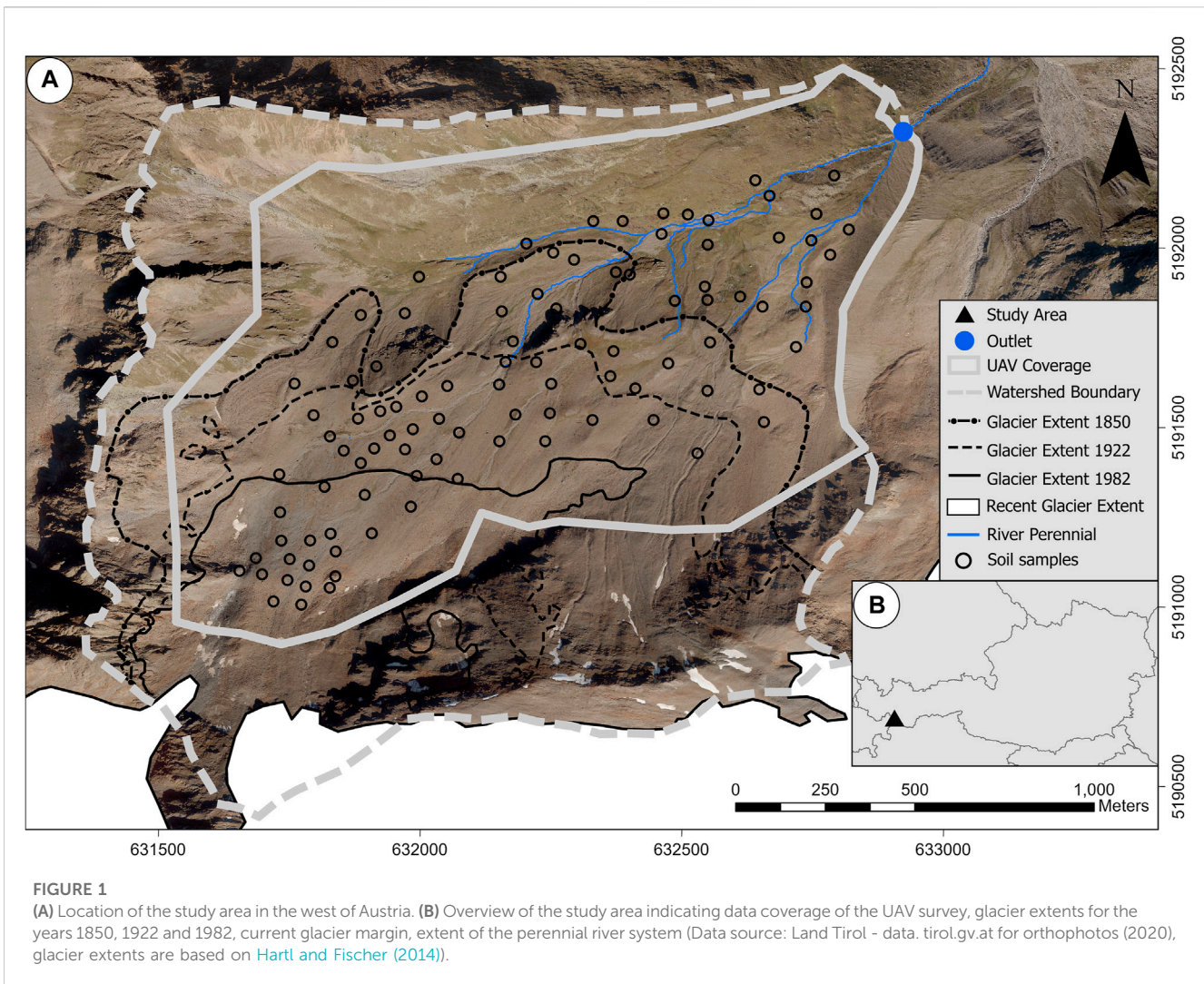
RQ3 How does geomorphic activity impact vegetation distribution at the catchment scale?.

## Study area

The Kaunertal Valley is a north-to-south oriented valley located in the Eastern European Alps in Tyrol, Austria (Figure 1A). This study focusses on a cirque-like hanging valley located on the orographic left side, west of the Upper Kaunertal Valley (Figure 1B), which was selected for its clear catchment borders, minimized elevation gradient to simplify vegetation composition assessment, reduced anthropogenic pressure, and distinct glacier dynamics compared to the main valley downslope. The Gepatschferner glacier, the second-biggest glacier in Austria, covers the south of this hanging valley. The study catchment is ~2 km<sup>2</sup> and has an elevation gradient from 2,400 m a.s.l. to 3,200 m a.s.l. As part of the eastern Alps crystalline zone, the area is geologically homogeneous, with mainly para- and orthogneis (Hammer, 1923). One-third of the catchment was ice-covered during the Little Ice Age (LIA) maximum extent. Since then, the glacier in the hanging valley has retreated approximately 1,500 m. More recent and detailed retreat rates are available for the glacier snout located in the main valley. In the Kaunertal Valley, mean annual retreat rates of 50 m have been observed since the year 2000 with a maximum of 125 m in 2017 (Kellerer-Pirklbauer, 2019). Remnants of moraines of advances and readvances for the years 1850, 1922 and 1982 allow a temporal classification of the area under investigation (Stocker-Waldhuber and Kuhn, 2019).

TABLE 1 Description of methods for multi-proxy-analysis of geomorphic activity.

	Method	Information	Captured processes	Includes erosion	Includes deposition	Observed/Potential change	Process intensity	(Potential) ecological disturbance	Level of measurement	Data source	Limitations	Example literature
Multi-proxy-analysis of geomorphic activity	SPI Stream Power Index	Measure of erosive power of flowing water determined by morphology	Fluvial incision, bank erosion, gully erosion	X		Potential for fluvial processes	Low to high intensity	Impede colonization, diversification	Metric	1 m DEM 2017 (Land Tirol data.gv.at)	Only covers processes in channels, activity for the full channel width challenging to determine	<a href="#">Heckmann and Vericat (2018)</a> , <a href="#">Moore et al. (1991)</a>
	SAI Sediment Accumulation Index	Thresholds below which sediment transfer is assumed to be stopped	Deposition of sediment		X	Potential for accumulation	Low to high intensity	Foster or impede colonization, diversification, reset	Metric	1 m DEM 2017 (Land Tirol data.gv.at)	Only relates to slope threshold in combination with SDI/SPI	<a href="#">Fryirs et al. (2007a)</a> , <a href="#">Fryirs et al. (2007b)</a>
	SDI Slope Denudation Index	Adopted slope length/steepness factor and erodibility factor for alpine areas	Potential for rill and interrill erosion	X		Potential for slope processes	Low to high intensity	Impede colonization, diversification	Metric	10 cm DEM 2019 <a href="#">Zangerl et al. (2022)</a> , 101 soil samples	Calculates only potentials, not necessarily calibrated for glacier forelands, influence of vegetation not covered	<a href="#">Schmidt et al. (2018)</a> , <a href="#">Schmidt et al. (2019)</a> , <a href="#">Cavalli et al. (2013)</a>
	DoD Digital elevation model of difference	Volumetric changes for 2006-2017	Debris flow, fluvial erosion and respective deposition	X	X	Observed surface change (definite time)	High intensity	Remove vegetation cover, reset colonization/succession	metric	1 m DEM 2006, 2017 (Land Tirol data.gv.at)	Small-scale process not covered, shows only temporal snapshot, distorted by snow fields, ground ice thawing	<a href="#">James et al. (2012)</a> , <a href="#">Sailer et al. (2012)</a>
Validation	GMM Geomorphic mapping	Erosion/deposition distinguishable, focus laid on high magnitude events with large extends	Fluvial erosion/deposition, debris flow erosion/deposition	X	X	Observed surface change (indefinite time)	High intensity	Remove vegetation cover, reset colonization/succession	Metric	Field survey 2021-2022	No temporal interpretation, small-scale processes are not covered, only qualitative not quantitative differentiation, producer bias	<a href="#">Otto and Dikau (2004)</a> , <a href="#">Eichel et al. (2013)</a>
	Plot sampling	Erosion/deposition distinguishable, focus laid on visible flow lines or deposition features	Fluvial erosion/deposition, debris flow erosion/deposition	X	X	Observed surface change (indefinite time)	Low to high intensity	Foster or impede colonization, diversification, reset	Metric	Field survey 2021-2022	Only qualitative not quantitative differentiation, producer bias	<a href="#">Kemppinen et al. (2021)</a>



During paraglacial adjustment, two dominant landforms emerge: (I) Drift-mantled slopes, which are closely associated with features such as lateral and terminal moraines, talus slopes, and debris flow channels and fans. (II) Glaciofluvial plains, distinctly characterized by incised channels, outwash deposits, and bank accretion ([Baewert and Morche, 2014](#)). On drift-mantled slopes, sediment reworking predominantly arises from slope wash processes, including rill, interrill, and gully erosion, as well as debris flows ([Dusik et al., 2019b](#); [Hilger et al., 2019](#)). On glaciofluvial plains, sediment reworking is mainly driven by bank erosion and fluvial deposition ([Geilhausen et al., 2013](#); [Hilger et al., 2019](#); [Morche et al., 2019](#)). Rockfall activity is predominantly confined to steep bedrock outcrops at high elevations, as delineated in the rockfall activity mapping by [Vehling et al. \(2019\)](#). Despite permafrost occurring on all slopes in the study area, as modeled by [Dusik et al. \(2019a\)](#), periglacial processes have limited significance in sediment denudation, with exceptions being dead ice melt near the current glacier extent and a distinct rock glacier in the western part of the study area. Additionally, there is no evidence of aeolian processes.

Associated moraine and till material is poorly sorted, with grain sizes ranging from silt to boulders, accompanied by weakly

developed soils, including (skeletal) Leptosols in recently exposed areas and a combination of (skeletal) Regosols and Cambisols in terrain that had been exposed for a longer duration ([Temme et al., 2016](#)).

Climatically, the study area is defined as a central-alpine dry region ([Fliri, 1975](#)). The meteorological station at Weissee (2,470 m. a.s.l.), 1.5 km west of the study area recorded a long-term mean annual air temperature of  $-0.05^{\circ}\text{C}$  (2007–2021) and mean annual precipitation rates ranging from 731 to 1,118 mm (data source: Tiroler Wasserkraft AG). Precipitation maxima occur during the summer months of July and August ([Haselberger et al., 2021](#)). Due to snow cover, the growing season for vegetation extends from mid-May until October. The area is above the local tree line and vegetation cover shows typical patterns of primary succession. Dominant species are *Cerastium uniflorum*, *Poa alpina* and *Veronica alpina* for early successional stages, *Salix herbacea*, *Poa alpina* and *Gnaphalium supinum* for mid-successional stages and *Nardus stricta*, *Cirsium spinosissimum* and *Poa alpina* for late successional stages (outside LIA-extent). Local shepherds use the hanging valley for grazing purposes for two to 4 weeks each August season. The analysis focuses on areas where UAV-derived vegetation data is available ([Figure 1A](#)).

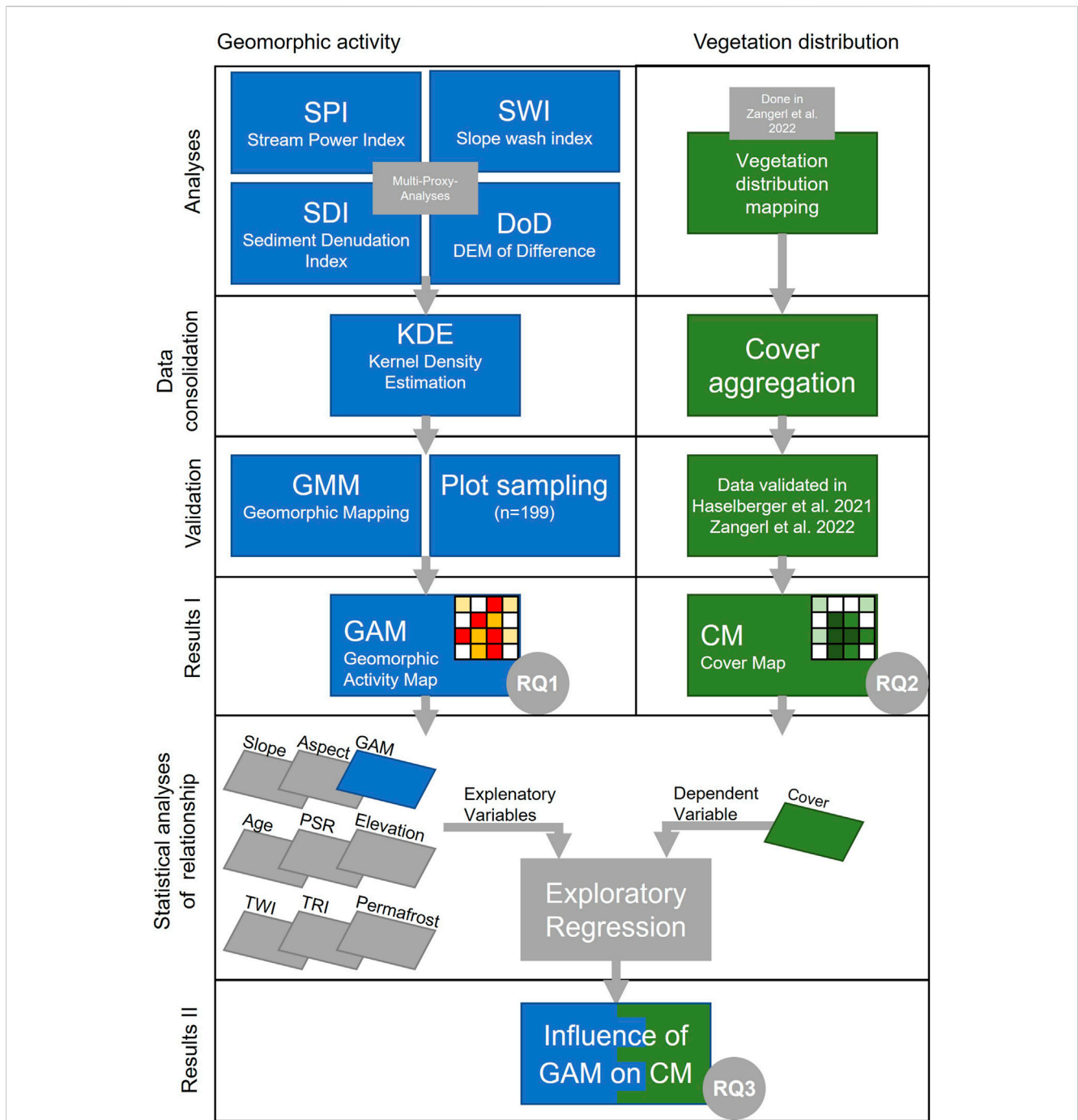


**FIGURE 2** Research design illustrating the methods utilized to address the three research questions: (I) Multi-proxy-analysis is employed to examine the distribution of geomorphic activity, (II) cover mapping is utilized to investigate vegetation distribution, and (III) statistical analyses are conducted to assess the impact of geomorphic activity and other site conditions on vegetation distribution as the dependent variable. Abbreviations not described in the figure: PSR - Potential Solar Radiation; TWI - Topographic Wetness Index; TRI - Topographic Roughness Index.

## Materials and methods

### Research design

In this study, geomorphic activity refers to the water-mediated transport of surface sediments on drift-mantled slopes and glaciofluvial plains, given the significant sediment reworking and

its impact on disrupting primary succession. Consequently, all bedrock areas identified through geomorphic mapping were excluded from the results.

We employed a multi-proxy analysis, integrating GIS-based techniques like the Stream Power Index (SPI), adapted Sediment Accumulation Index (SAI), adapted Slope Denudation Index (SDI), and a Digital Elevation Model of Difference (DoD) (Table 1). This

data informed the creation of a Geomorphic Activity Map (GAM) through a kernel density function, subsequently validated through geomorphic mapping and plot sampling (RQ1).

We processed high-resolution vegetation data to construct a catchment-scale map depicting vegetation cover and stability thresholds (RQ2). These two maps were subsequently harmonized, followed by an exploratory regression analysis aiming to scrutinize the impact of geomorphic activity on vegetation cover (RQ3).

A visual summary of the research design is presented in [Figure 2](#).

## Geomorphic activity based on a multi-proxy-analysis

**SPI:** Stream Power Index (SPI) is a measure of the potential erosive power of water ([Moore et al., 1988](#)). It is calculated as the product of slope angle and the upslope contributing area. SPI calculation was performed on DEM1 in ArcGIS Pro 2.7. The results were cross-checked with the GMM, and values exceeding the 90th percentile were classified as potentially exhibiting geomorphic activity.

**SAI:** Areas with a high potential for sediment accumulation were identified based on the sediment disconnectivity approach by [Fryirs et al. \(2007a\)](#). All contiguous pixels with a slope threshold  $<15^\circ$ , directly connected to potential flow lines obtained in the SPI analyses, were classified as potentially geomorphologically active, as suggested by [Nicoll and Brierley \(2017\)](#).

**SDI:** SDI was used for estimating potential for sheet and rill erosion based on the erodibility of substrate and the slope position. The erodibility factor was calculated based on [Schmidt et al. \(2018, 2019\)](#), who adapted the parameter for steep alpine terrains. Substrate properties stem from topsoil samples collected at 101 sites ([Figure 1B](#)), examined for fine sand, silt, and clay using a Retsch La-950 analyzer. Organic matter content was determined by loss on ignition. Stone cover ( $\geq 4$  mm grain sizes) was gauged within 1x1m plots at sample locations, for adjusting the erodibility factor ([Poesen and Lavee, 1994](#)). Point calculations of erodibility were spatially interpolated with Empirical Bayesian Kriging ([Krivoruchko, 2012; Krivoruchko and Gribov, 2019](#)) in ESRI Arc GIS Pro 2.7 using four environmental covariates: elevation, aspect, curvature, and geomorphic process groups ([Bishop and McBratney, 2001](#)). The slope position was based on the slope-length and slope-steepness ([Moore et al., 1991](#)) which were calculated in SAGA GIS 8.1.1 ([Conrad et al., 2015](#)), based on the alpine equation proposed by [Schmidt et al. \(2019\)](#) and using a 1 m Digital Elevation Model (DEM1; Land Tirol, data. tirol.gv.at). Maximal flow length was limited to 100 m, due to high infiltration, and an aggregated equation for steep slopes was applied ([Schmidt et al., 2019](#)). The results were cross-checked with the geomorphic mapping (GMM), and values above the catchment mean were classified as potentially exhibiting geomorphic activity.

**DoD:** To determine real surface changes, a DEM of Difference (DoD) was computed, utilizing DEM1 from the year 2006 with a vertical accuracy of 0.15 m and a 0.5 m resolution DEM (DEM05) from 2017 with a vertical accuracy of 0.1 m. Both datasets are based on LiDAR campaigns of the Federal Government of Tirol (Land Tirol, data. tirol.gv.at) and were resampled to 1 m grid size. Following [Lane et al. \(2003\)](#) and [James and Robson \(2012\)](#), we calculated a minimum level of detection of 0.18 m for the DoD. After

visual inspection of the results, the minimum level of detection was raised to 0.4 m. This conservative approach aimed to minimize errors from insufficient vegetation filtering and subsequent distorting effects of growing shrubs. Based on the geomorphological field mapping, significant elevation changes resulting from rock glacier and dead ice thawing as well as glacier retreat were excluded from the DoD ([Figure 5](#)).

**Data consolidation:** The results from SPI, SAI, SDI, and DoD analyses ([Figure 5](#)) were normalized to a 0–1 scale. For each method, raster data were converted to point data by selecting only raster cells with classified activity. Each point retained the value calculated by its respective method. A smoothed raster for each method was then produced using kernel density estimation. Smoothing rasters is beneficial since the extent of geomorphic activity varies with varying magnitudes and frequencies throughout a landscape ([Cox, 2007](#)). GMM detects activity if any of the four methods show activity within a 20 m radius. The radius choice results from aligning SPI, SAI, SDI, and DoD rasters with channel widths from the GMM using iterative adjustment. A weighted overlay of the four rasters combines data, factoring in method observation intensity, privileging higher values (e.g., SPI) in results. GAM results represent the probability of geomorphic activity within an area, ranging from 0 to 1. Increased probability arises from the alignment of multiple methods indicating activity in the same area and/or a single method exhibiting high intensities in an area.

**Validation:** The mapping of the glacier foreland geomorphology was conducted according to protocols outlined by [Smith et al. \(2013\)](#) and [Chandler et al. \(2018\)](#). Mapping was prepared by interpretation of orthophotos (Land Tirol - data. tirol.gv.at) and DEM1 derivatives. Based on GAM results, we randomly selected 100 plots deemed to be disturbed, and 99 plots deemed to be undisturbed. For locations with water, bedrock or ice surface, as well as inaccessible steep scree and bedrock slopes, we took predefined alternative sample locations. The preliminary mapping of the remotely-sensed data was verified through field mapping in summers 2021 and 2022 Landscape interpretation was supported by results published in [Heckmann et al. \(2019\)](#). Glacier extents are based on [Hartl and Fischer \(2014\)](#), and were refined by field observations and supported by digital terrain representations. Processes and landforms were mapped, including areas of fluvial erosion and deposition, debris flow erosion and deposition, and active talus slopes. Plot based validation was done in 1x1 m plots, recording the presence or absence of geomorphic activity based on visible flow lines, accumulated sediment, and freshly eroded rock fragments. Validation plots included the 101 plots for soil sampling and additional 98 plots.

## Mapping of vegetation cover

High-resolution distribution of vegetation is based on vegetation presence and absence with a resolution of 10 cm based on UAV-remote sensing orthoimages, classified with a random forest algorithm adopted from [Zangerl et al. \(2022\)](#). For this study, we aggregated this vegetation data to calculate cover thresholds at a 1 m scale. The percentage of vegetation cover within a 1x1 m area was classified to estimate the stage of biogeomorphic succession, which is associated with cover thresholds ([Martin et al., 2010; Eichel et al., 2016; Haselberger et al., 2021](#)). Classes ranged from  $<35\%$  cover (low stability, highly geomorphologically

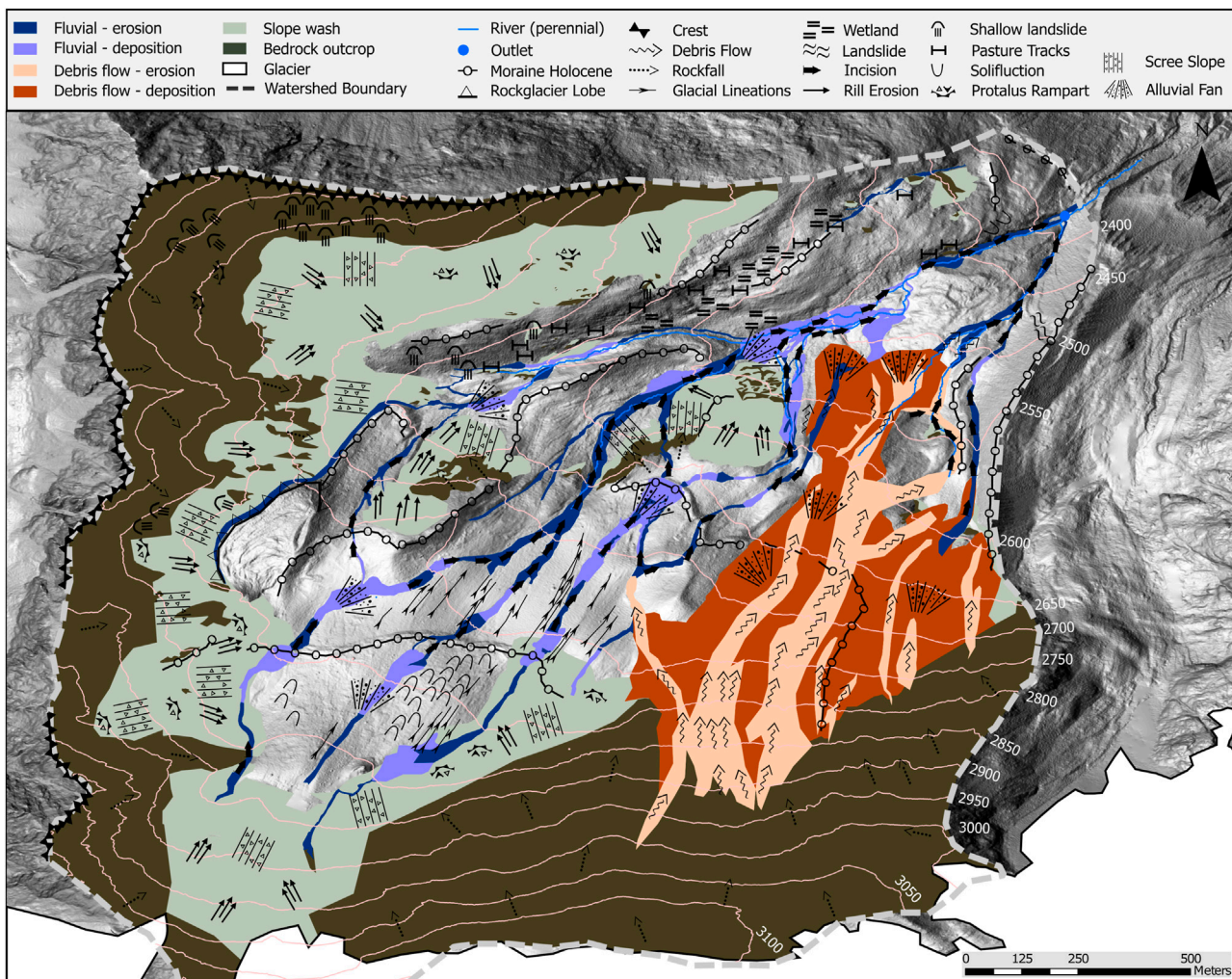


**FIGURE 3**  
 Map illustrating the geomorphic landforms and processes of the study area. This includes locations of fluvial erosion and deposition, debris flow activity, areas of slope wash, and bedrock outcrops. Subsequent results will exclude bedrock outcrop areas since rockfall processes are not addressed in the multi-proxy analyses. Zones without a distinct signature exhibited no significant signs of geomorphic activity during field observations. Field mapping was conducted in the summers of 2021 and 2022. Landscape interpretation was augmented by remotely sensed data and insights from [Heckmann et al. \(2019\)](#).

active), 35%–75% (moderately stable and active) and >75% (stable, inactive) based on [Haselberger et al. \(2021\)](#).

### Site conditions and exploratory regression

To determine the influence of GAM on vegetation cover, it was necessary to disentangle GAM from other site conditions. Additional site conditions, that affect plant growth, were collected: ground ice distribution is based on a model by [Otto et al. \(2020\)](#). Elevation as well as other DEM1 derivatives including slope angle, aspect, potential solar radiation (PSR), surface roughness (TRI, [Moore et al., 1991](#)) and topographic wetness index (TWI, [Beven and Kirkby, 1979](#)) data were derived using ArcGIS Pro 2.7 (data source Land Tirol, data. tirol.gv.at).

Exploratory regression analysis ([Braun and Oswald, 2011](#)) was used to identify the factors among eight explanatory variables (elevation, slope, TRI, TWI, GAM, radiation, ground ice distribution, and terrain age) that influence vegetation cover. Regression outputs are ranked according to Pearson’s correlation coefficients. To distinguish between first-order influence of primary explanatory variables and the second-order influence of GAM, we examined residuals from the global ordinary least squares (OLS) regression. Residuals of the first order regression exceeding 1.5 standard deviations in the OLS model identified areas where GAM potentially influences vegetation cover. The contrast in GAM values within and outside these areas was statistically assessed through the Wilcoxon–Mann–Whitney test ([Wilcoxon, 1947](#)) using the R package ggpubr ([Kassambara and Kassambara, 2020](#)).

**TABLE 2 Validation of GAM (Geomorphic Activity Map) with GMM (Geomorphic Mapping) and plot survey.**

Validation of GAM with GMM							
Group	GMM area [m <sup>2</sup> ]	Proportion of catchment [%]	GAM area <sup>†</sup> [m <sup>2</sup> ]	Overlap (GMM+GAM) [m <sup>2</sup> ]	False positive GAM <sup>†</sup> [%]	False negative GAM <sup>†</sup> [%]	Correctly covered GAM [%]
All	572,35	36.4	631,09	413,91	37.6	27.6	75.3
Inside LIA extent	360,21	47.2	357,99	253,28	19.3	14.5	82.1
Fluvial erosion	64,90	4.8	-	59,73	-	-	92.0
Fluvial deposition	52,23	3.9	-	47,67	-	-	91.3
Debris flow erosion	78,08	5.8	-	57,90	-	-	75.2
Debris flow deposition	146,60	10.9	-	93,88	-	-	66.2
Slope wash erosion/ deposition	173,29	13.1	-	131,35	-	-	75.8
Validation of GAM with plot survey							
Plots [n]	Observed as active plots [n]	Observed as inactive plots [n]	Correctly covered GAM [n]	Correctly covered GAM [%]			
199	100	99	171	85.9			

Distribution of vegetation cover.

## Results

### Multi-proxy-analysis of geomorphic activity

Geomorphic mapping revealed that fluvial processes predominated on the gently sloping glaciofluvial plains, particularly near the catchment’s outlet point. In contrast, debris flow and slope wash processes were observed on drift-mantled slopes, and rockfall activity was evident along the outer margins of the catchment, especially in proximity to the current glacier extent. These observations underscore the dominant processes responsible for sediment reworking (Figure 3).

In the southwest of the catchment, the glaciofluvial plain is mostly flat, consisting of a braided fluvial network with shallow, periodically active channels that alternate between erosion and deposition. Perennial flow starts between the 1850 and the 1922 terminal moraines, where a distinct 50-m-high step in the terrain divides the study area into an upper and a lower part. From here, the transport capacity of the channel increases, this is reflected by the deposition of larger blocks further downstream on the glaciofluvial plain. The step in the terrain also leads to active slope wash processes and the steep drift-mantled slopes.

On drift-mantled slopes in the southeast, debris flow channels, bordered by levees, lead to debris fans that reach near the outlet point. Channels are assumed active during snowmelt and intense rainfall events, linking the uppermost slopes to the cirque floor. A spectrum of channels, ranging from recently active ones characterized by unweathered deposits to abandoned channels showing signs of weathering and erosion, highlights the variability in local

geomorphic activity over time. Due to the high transport capacity, deposited sediments cover large areas (Table 2).

Bedrock outcrops dominate the higher elevated borders of the catchment in the southern and western parts, near the current glacier margin and on two small bedrock outcrops in the center of the catchment. Associated with these rock slopes are talus slopes, which show a sequence of erosional and depositional features. Talus slopes act as buffers for rockfalls from above, ensuring eroded rock fragments are retained on these slopes and do not extend to the glaciofluvial plain.

SPI values exceeding the 90th percentile indicate geomorphic activity within both perennial and episodic channel networks (Figure 4). SAI highlights geomorphic activity through sediment accumulation, predominantly on the glaciofluvial plain. SDI values surpassing the catchment average show geomorphic activity mainly on steep sediment-mantled slopes and the fluvial network spanning the glaciofluvial plain. DoD shows geomorphic activity through sediment accumulation in areas of fluvial deposition and some debris flow channels, as well as by detecting erosion fluvial channels, and less distinct in debris flow channels and steep sediment-mantled slopes.

The GMM indicates that 36.4% of the study area are geomorphologically active (Figure 3; Table 2). For the entire catchment, GAM accurately mapped 75.3% of this active area, and 82.1% within the LIA moraine (Figure 5). It correctly covered 92.0% of fluvial erosion and 91.3% of fluvial deposition. Debris flow erosion, observed on steep slopes and channels, was correctly identified on 75.2% of the area. Debris flow deposition had a marginally reduced accuracy with 66.2% coverage. GAM accurately represented slope wash processes, which include erosion and deposition on drift-mantled slopes, on 75.8% of the area. Validation of the GAM results

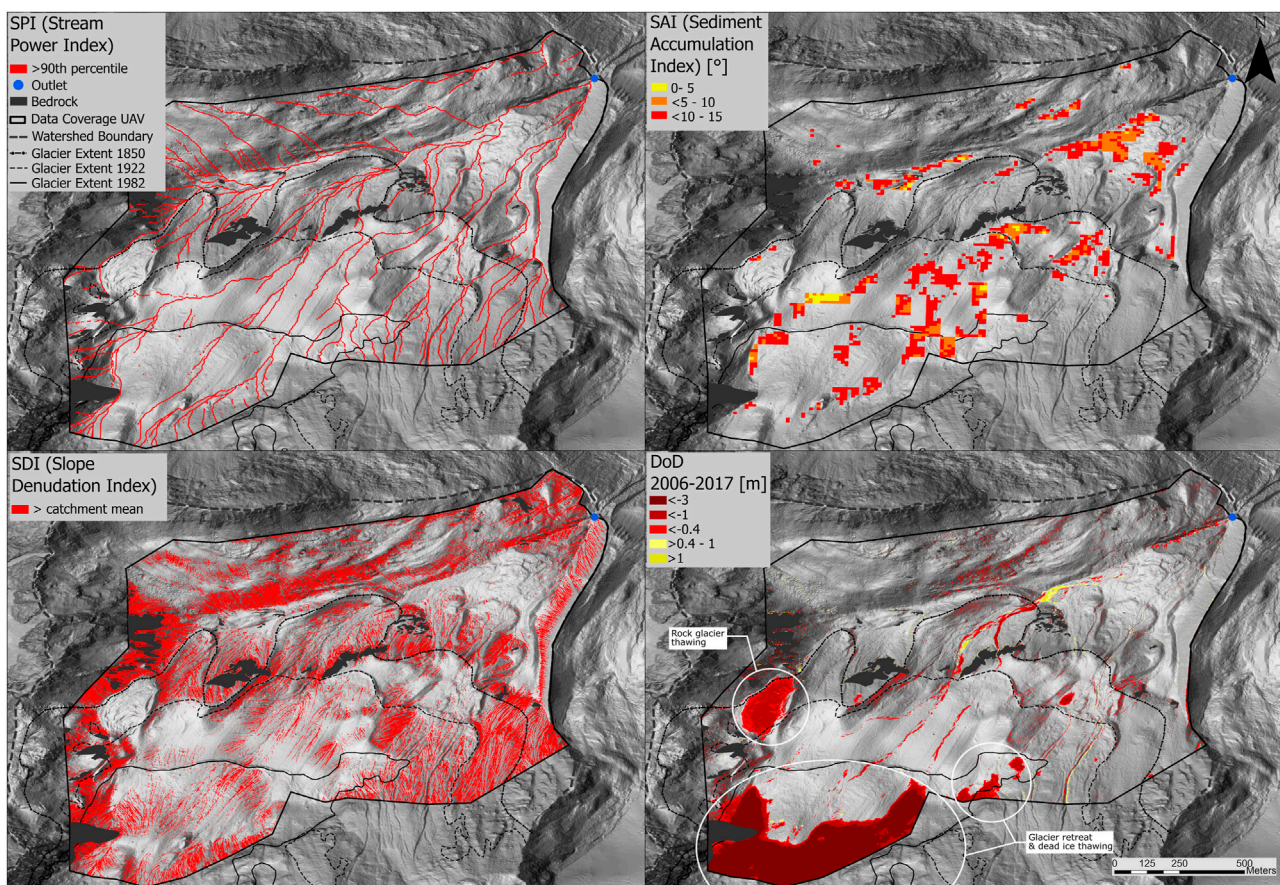


**FIGURE 4** Individual results from the multi-response analyses, representing the methods incorporated to produce the final activity map. SPI illustrates fluvial processes within channels, linked to flow accumulation and slope. SAI emphasizes sediment accumulation, associated with upslope contributing area and abrupt changes in slope. SDI highlights erosion and gravitational processes associated with slope length and steepness and substrate erodibility. DoD displays the actual surface change in meters over 12 years. Changes related to rock glacier thawing, glacier retreat, and dead ice thawing were omitted from the DoD.

through plot-based analysis showed that 85.9% of the presence or absence of geomorphic activity was correctly classified by the model. The GAM indicates the highest probability of geomorphic activity within the glaciofluvial plain and on steep drift-mantled slopes. This observation is in line with field mapping results with zones of increased potential activity in areas where fluvial erosion and deposition, slope wash activity and debris flow occurrence has been mapped.

Vegetation predominantly covers the central and northern areas of the study site. A vegetation gradient is evident, with low cover near the current glacier extent and maximal cover towards the cirque’s outlet (Figures 5A, B). Early colonizing plants create the first small (~2 m<sup>2</sup>) patches of high vegetation cover close to the glacier margin. The first larger patches (~100 m<sup>2</sup>) of high cover (>75%) occur about 50–80 years after glacier retreat. In areas that have been glacier-free for over 100 years, patches of vegetation significantly increase in size (~5,000 m<sup>2</sup>) and number.

These patches predominantly exist on the glaciofluvial plain near periodic water sources. On terrains younger than 100 years, fluvial deposition areas first achieve a 35% vegetation cover (Figure 6C). In terrain aged between 100 and 170 years, certain areas of fluvial deposition surpass the 75% cover threshold. Beyond the LIA moraine, the periodically active sections of the glaciofluvial

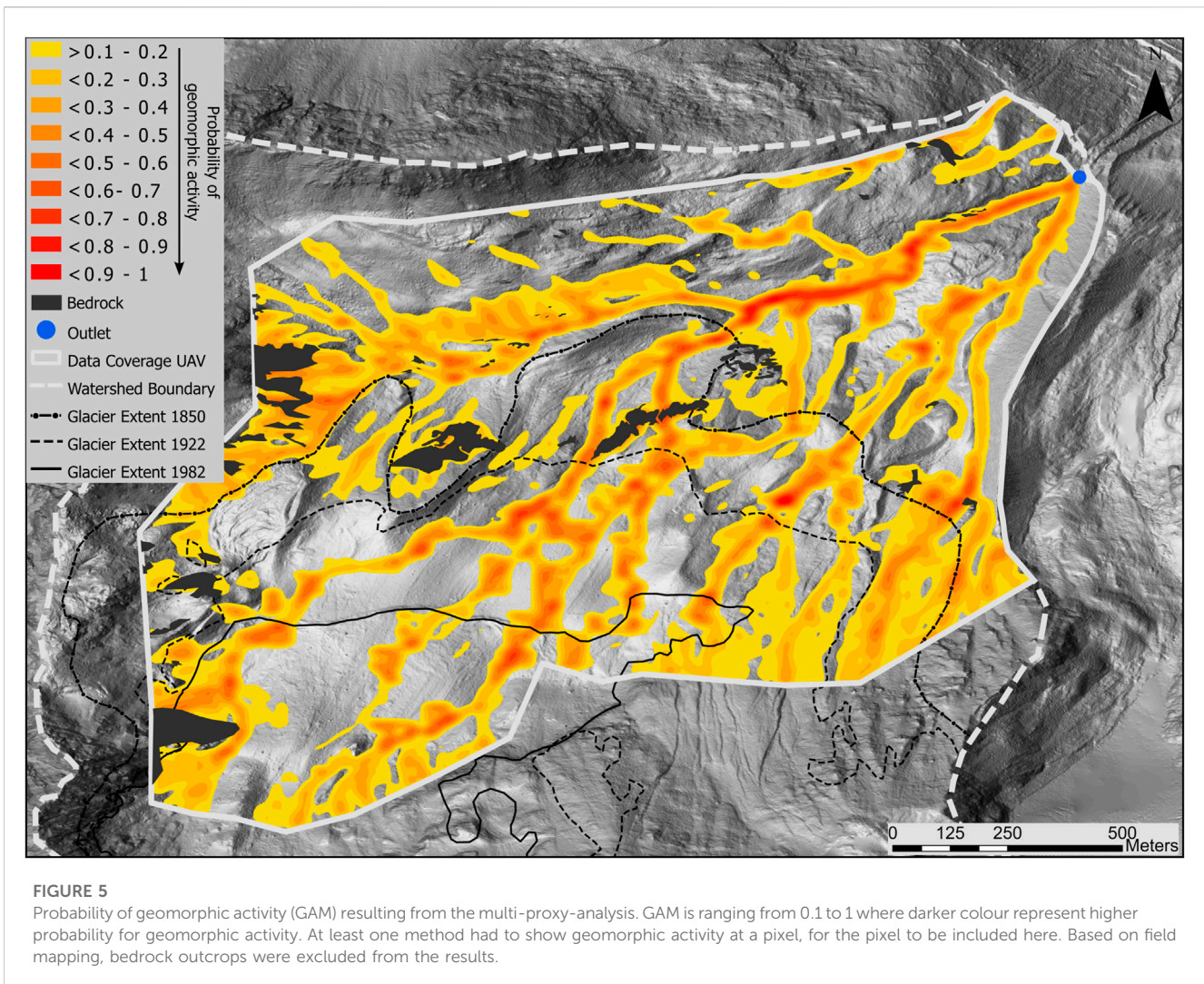
plain are densely vegetated, except for extensive sediment aggradation zones, which display limited to no vegetation.

Areas susceptible to debris flows start to exhibit vegetation cover above the threshold of 35% only outside the LIA boundary. Here, depositional areas of debris flows display high vegetation cover, with some areas surpassing the 75% thresholds. In general, areas affected by debris flow erosion exhibit considerably lower vegetation cover.

On drift-mantled slopes with signs of erosion and slope wash, vegetation is sparse on terrains younger than 100 years; these areas are mostly talus slopes linked to high-elevation rock outcrops. In terrains glacier-free for 100–170 years, slope wash is predominantly observed on moraine landforms. While vegetation becomes denser in these areas, regions beyond the LIA border primarily exceed the 35% cover, occasionally exceeding 75%.

### Influence of abiotic factors including geomorphic activity on vegetation distribution

Elevation, solar radiation, and terrain age serve as primary explanatory parameters for understanding vegetation distribution



(Model 7, adjusted R-squared = 0.47, AIC = 143161.6, VIF = 1.75). Two additional models, which have comparable explanatory power, include the same parameters as model 7 along with an additional parameter, one including GAM (model 12, adjusted R-squared = 0.46, AIC = 139393.99, VIF = 1.75) and one including TWI (model 10, adjusted R-squared = 0.46, AIC = 120484.19, VIF = 1.79). Due to the interrelatedness of input data, the results showed significant correlation between GAM and topographic wetness index (TWI) ( $p < 0.001$ ,  $R^2 = 0.45$ ). Higher elevation was negatively associated with vegetation distribution, while higher radiation and terrain age were positively associated. In addition, high results of both TWI and GAM were found to have a negative association with plant distribution. Results for 12 additional model combinations can be found in the (Supplementary Table S1). The low variance inflation factor values observed for each predictor variable in the models indicate that multicollinearity was not a significant issue. Spatial autocorrelation of model results was high, as indicated by Moran's I of 0.88 and  $p < 0.001$ .

The residuals from Model 7 highlight areas where first order explanatory variables—elevation, solar radiation, and terrain age—do not account for the vegetation distribution (Supplementary Figure S6). Wilcoxon-Mann-Whitney showed significantly higher GAM values for areas with high positive ( $> 1.5$  standard deviations,

$p < 0.001$ ;  $W = 1.32e+10$ ,  $n_1 = 25\ 852$ ,  $n_2 = 898\ 589$ ) and high negative ( $< -1.5$  standard deviations,  $p < 0.001$ ;  $W = 1.07e+10$ ,  $n_1 = 19\ 612$ ,  $n_2 = 898\ 589$ ) residuals.

## Discussion

### Multi-proxy-analysis of geomorphic activity

We combined a GIS-based approach of different proxies representing geomorphic activity to produce a geomorphic activity map (GAM).

Fluvial processes are best represented by the multi-response approach, which is explained by the fact, that all four proxies are able to depict processes occurring within channels and two of them are explicitly based on a flow algorithm, namely, SPI and SDI. GAM results indicate a high probability of geomorphic activity along fluvial flowlines, while the likelihood decreased towards the banks of the channel, which corresponds to peak erosion and transport capacity midstream (Gurnell et al., 2012). While banks and floodplain are less likely to be affected, high-magnitude processes can still impact a broader cross-section of the channel (Gurnell et al., 2000; Gentili et al., 2010). Assessing

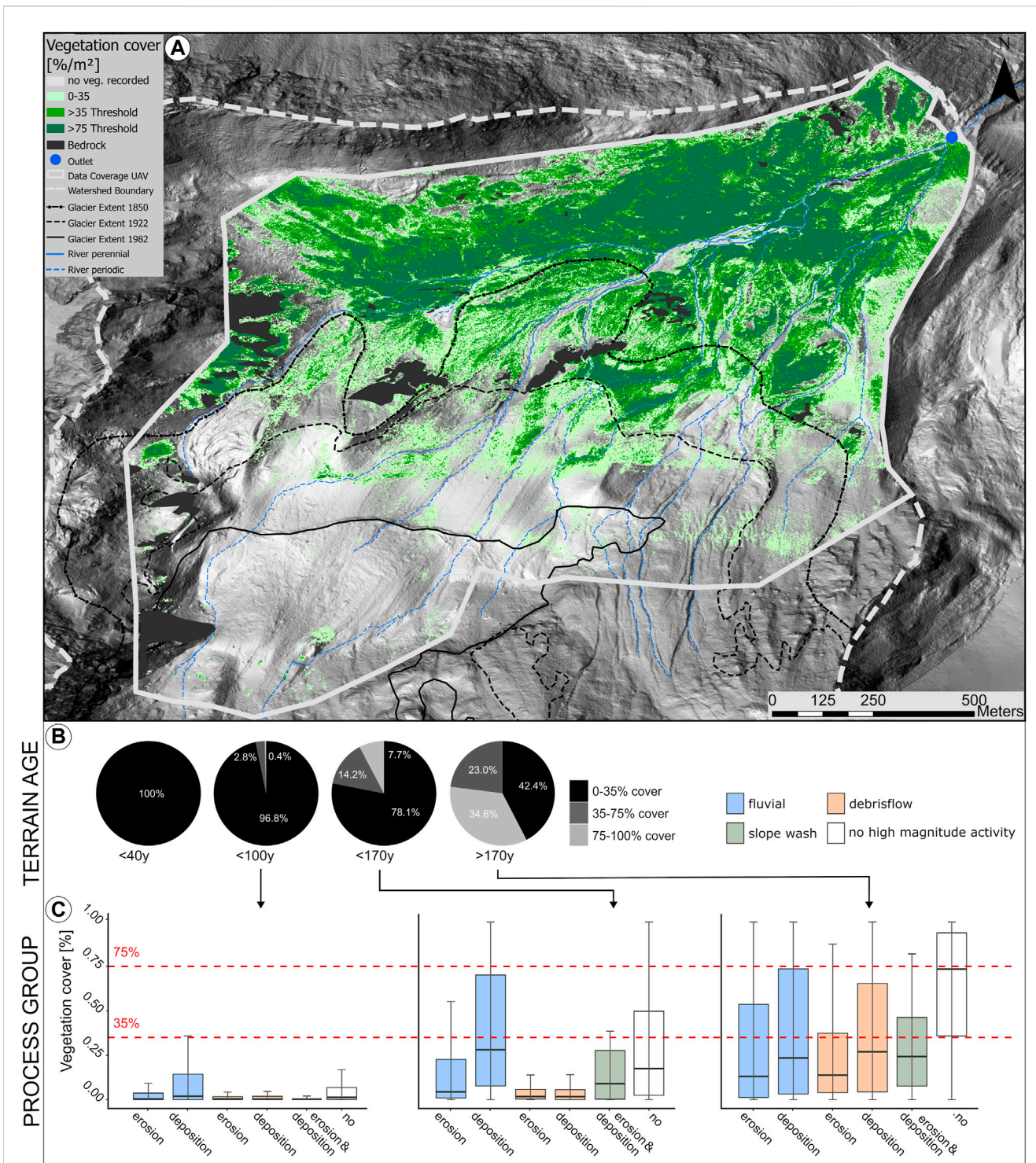


**FIGURE 6** Distribution of vegetation cover based on three stability classes: <35%, >35–75%, and >75% (Haselberger et al., 2021), presented for the catchment (A), per terrain age (B), and process group (C). Data on vegetation distribution is based on high-resolution UAV data (Zangerl et al., 2022), glacier extents are based on Hartl and Fischer (2014), and geomorphic process groups are based on GMM. For the boxplots the upper and lower box margins mark the 75th and 25th percentile, respectively, with the line in the center showing the median and the black dots showing the mean. The whiskers indicate the minimum and maximum values, except for outliers.

channel width coverage for both fluvial and debris flow processes remains a significant hurdle in catchment studies (Ferrer-Boix et al., 2016). Although our method provides a generalized way to determine channel width, it still captures the varying disturbance

potentials of different magnitudes of fluvial events in relation to the channels cross profile.

The SDI highlighted activity zones on drift-mantled slopes due to the pronounced relief energy in these regions, but detailed

representation posed difficulties for various reasons: (I) While slope wash processes are evident on talus slopes, they intersect with rockfall-induced erosion and deposition, particularly in the southwest where elevated rock outcrops influence these slopes (Vehling et al., 2019). (II) Erosion on drift-mantled slopes occurs in channels the resolution of our data cannot capture (Dusik et al., 2019b). Erosional features' spatial and temporal variability complicates this further (Dühnforth et al., 2007; de Haas et al., 2018). (III) Sediment deposition on drift-mantled slopes contrasts with glaciofluvial plains, as sediment predominantly accumulates on steeper slopes (Vehling et al., 2019), which is not covered by SAI. (IV) Our data, capturing a singular topographic situation, emphasizes active debris flow channels, often neglecting dormant ones. The complexity of potential channels yields diffuse sediment in coalescing debris fans (Carrivick and Heckmann, 2017), complicating the depiction of the entire range of channel activity and linked deposition.

The disparity between SAI and DoD values arises from the fact that SAI represents potential sediment accumulation areas based on process magnitudes observed in the DoD. This means that while SAI may depict sediment accumulation for magnitudes exceeding the DoD's minimum detection level, it identifies areas most likely to experience sediment disturbance that the DoD does not account for. Despite these remaining challenges, the introduced multi-response method provides a catchment-wide identification of potential geomorphic activity. While numerous approaches can describe geomorphic processes with greater detail—ranging from qualitative descriptions (Otto et al., 2009; Geilhausen et al., 2012) and surface change quantifications for specific landforms (Dusik et al., 2019b; Hilger et al., 2019; Morche et al., 2019), to modeling efforts on erosion (Meusburger et al., 2010), fluvial dynamics (Hodgkins et al., 2003), debris flows (Haas et al., 2012), rockfall (Heckmann et al., 2016a), or sediment connectivity simulations (Cavalli et al., 2013)—our method deliberately simplifies for broader applicability. While this approach may compromise on accuracy, it provides a comprehensive catchment-scale perspective, a view essential for discerning scale dependencies in biogeomorphic processes shaping the mosaic landscape of glacier forelands.

Integrating advanced numerical models related to debris flow and rockfall processes as well as different approaches to sediment accumulation on the glaciofluvial plain and drift-mantled slopes will be a valuable next step in refining the accuracy and broadening the applicability of this multi-response approach.

## Distribution of vegetation cover

The observed mosaic of different levels of vegetation cover on smaller scales shows two key factors of allogenic influence: local site conditions that constrain plant growth and the perturbing effect of geomorphic activity (Wojcik et al., 2021). The observed large-scale gradient of increasing vegetation cover, terrain age, and elevation has been well-documented (Matthews, 1992; Körner, 2003; Raffl et al., 2006; Gentili et al., 2010). However, traditional plot-based surveys often overlook the influence of geomorphic processes, as focus is laid on preferably stable plot locations (Cutler et al., 2008a; Cutler, 2010).

Initial patches of vegetation along fluvial channels represent locations of early colonizers that act as the nucleus for the next stage of plant growth (Jumpponen et al., 1999; Matthews and Water, 2015). Specifically in areas of fluvial deposition,

geomorphic processes provide resources such as water and fine sediment as a substrate for initial plant growth (Miller and Lane, 2018; Kemppinen et al., 2021). This observed pattern is explained by the role of “geomorphic-pulses”—processes that provide resources, including water and fine-grain substrate, for early colonization (Gurnell et al., 2000; Miller and Lane, 2018; Larsen et al., 2020). In these areas, periphyton, a submerged mixture of algae, microbes, and detritus, serves as potential pioneer organisms that facilitate subsequent colonization by vascular plants, a group of organisms, which is indicative for intermediate rates of fluvial processes (Roncoroni et al., 2019). With time, these patches gradually coalesce to form larger, more uniform areas of dense vegetation (Cutler et al., 2008b). Once they exceed stability thresholds, they can effectively reduce small-scale sediment transport (Haselberger et al., 2021; Ohler et al., 2023), which seems to first occur in proximity to flowlines on the glaciofluvial plain (Miller and Lane, 2018; Cienciala et al., 2020).

In contrast, debris flow areas reflect the importance of time since the last geomorphic disturbance for plant colonization (Lane et al., 2016). In the debris flow channels we observed, varying levels of plant cover were evident. This variation in vegetation cover likely reflects the time since the last debris flow event in each respective channel, given the consistent topography. Abandoned channels can even serve as refuge habitats for plant colonization due to variations in soil moisture and grain size, as observed by (Gentili et al., 2010). Higher cover values in depositional portions of the debris flow network indicate that only few high magnitude events reach all the way to the lower areas of the fan (Lane et al., 2016), exemplifying the importance of process magnitude in altering plant colonization.

In areas without debris flow processes, drift-mantled slopes exhibited a progressive increase in vegetation cover associated with terrain age and elevation. The absence of high-magnitude disturbance events, such as landslides, deep gully erosion, and rock avalanches, may facilitate gradual colonization (Eichel et al., 2016). This aligns with the notion that low to intermediate disturbances do not completely reset successional stages, allowing specialized species to adapt (Stawska, 2017; Wojcik et al., 2020; Eichel et al., 2023) and biogeomorphic succession tends to follow an idealized shift from abiotic to biotic dominance.

## Influence of abiotic factors including geomorphic activity on vegetation distribution

The exploratory regression analysis in this study supports the visual interpretation of the vegetation cover. The patchiness of succession is also shown by the spatial autocorrelation results of the OLS model, which show that adjacent locations are more similar in biotic and abiotic parameters (Junker et al., 2020). Commonly terrain age, elevation, and greater exposure to sunlight are seen to have a landscape-scale influence on vegetation distribution (Gentili et al., 2010; Robbins and Matthews, 2018; Fischer et al., 2019), which was supported by our results. Our exploratory regression analysis confirms the notion that disturbances caused by geomorphic activity as second order factor that either limit plant colonization, or provides necessary pulses after which colonization can intensify

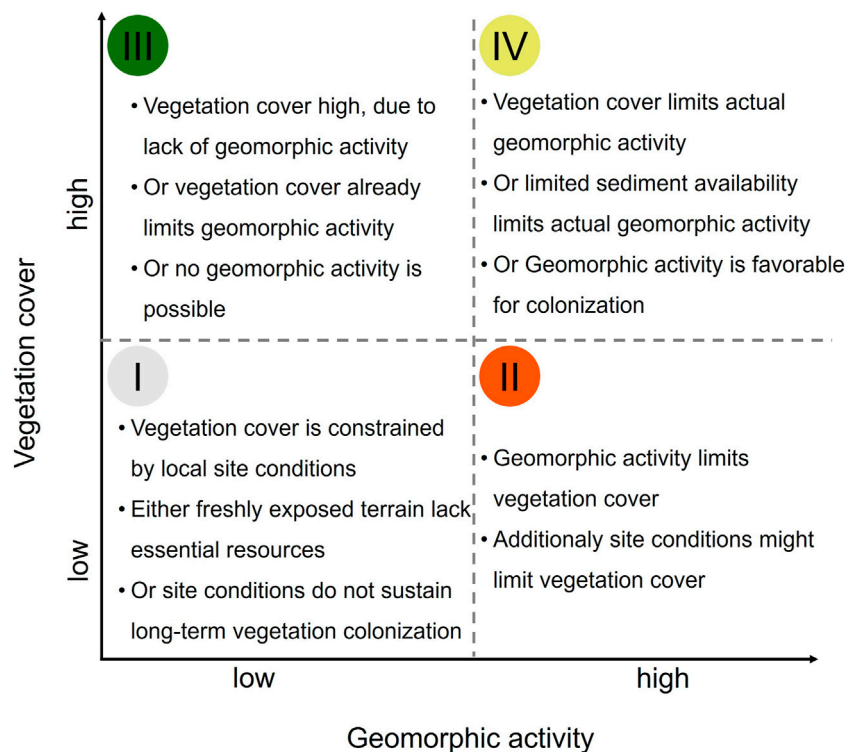


**FIGURE 7**  
Possible situations for the interaction of GAM with vegetation cover. The four potential relationships between the potential for high geomorphic activity and actual vegetation cover present relate to stages during biogeomorphic succession. Potential causes for each of the four situations are listed in the respective quadrant, which relate the current state to successional pathways.

(Larsen et al., 2020), which is responsible for spatial heterogeneity in successional stages in our catchment (Wojcik et al., 2021).

Although our multi-proxy approach proved to be valuable for interpreting landscape patterns of vegetation distribution, the predictive power of GAM is limited for two reasons: (I) Vegetation cover can be high despite a high potential for geomorphic activity. For example, on the densely vegetated south facing slopes, which showed high geomorphic activity. Here, GAM represents potential geomorphic activity and does not provide information on the actual situation in the field. (II) Vegetation cover can be low in areas with limited resources despite low levels of geomorphic activity, for example, in areas with a young terrain age and a lack of nutrients (Schmidt et al., 2016).

Synthesis: A time-independent framework for understanding the relationship between geomorphic activity and vegetation distribution.

From a comprehensive catchment-wide analysis of geomorphic activity and plant cover distribution thresholds, several key observations emerge.

- High magnitude geomorphic processes, such as fluvial and debris flow processes can reset biogeomorphic succession.
- These processes occasionally interrupt the gradual transition from abiotic to biotic dominance during biogeomorphic succession. As a result, terrain age may not always be a reliable indicator. Instead, the time since the last significant disturbance becomes more relevant.

- Initial colonization opportunities might arise not only from periods of reduced disturbance but also from essential geomorphic pulses facilitating early colonization phases.
- Some regions, despite displaying no evident geomorphic activity, might maintain sparse vegetation due to resource limitations.
- In areas where topography indicates heightened geomorphic activity, dense vegetation could be indicative of historical slope stabilization by plant life.

Based on these observations Figure 7 offers a time-independent conceptual summary of the interaction between geomorphic activity and vegetation cover, featuring four potential situations derived from this study’s results and previous research on the topic (Matthews, 1992; Viles et al., 2008; Eichel et al., 2016; Lane et al., 2016; Miller and Lane, 2018; Wojcik et al., 2021).

While the conditions of these scenarios are well understood, the framework allows assessment of biogeomorphic succession based on geomorphic activity and vegetation cover, irrespective of time, considering the spatial complexity at the catchment scale as demonstrated in this study. A simple overlay of GAM and the vegetation cover map allowed us to map the spatial distribution of the four situations in the research area (Figure 8), which is further illustrated using aerial snapshots as examples (Figures 8A–H). This spatial delineation of four stages in biogeomorphic succession provides a foundation for subsequent studies to delve deeper into the functional aspects of geomorphic processes and

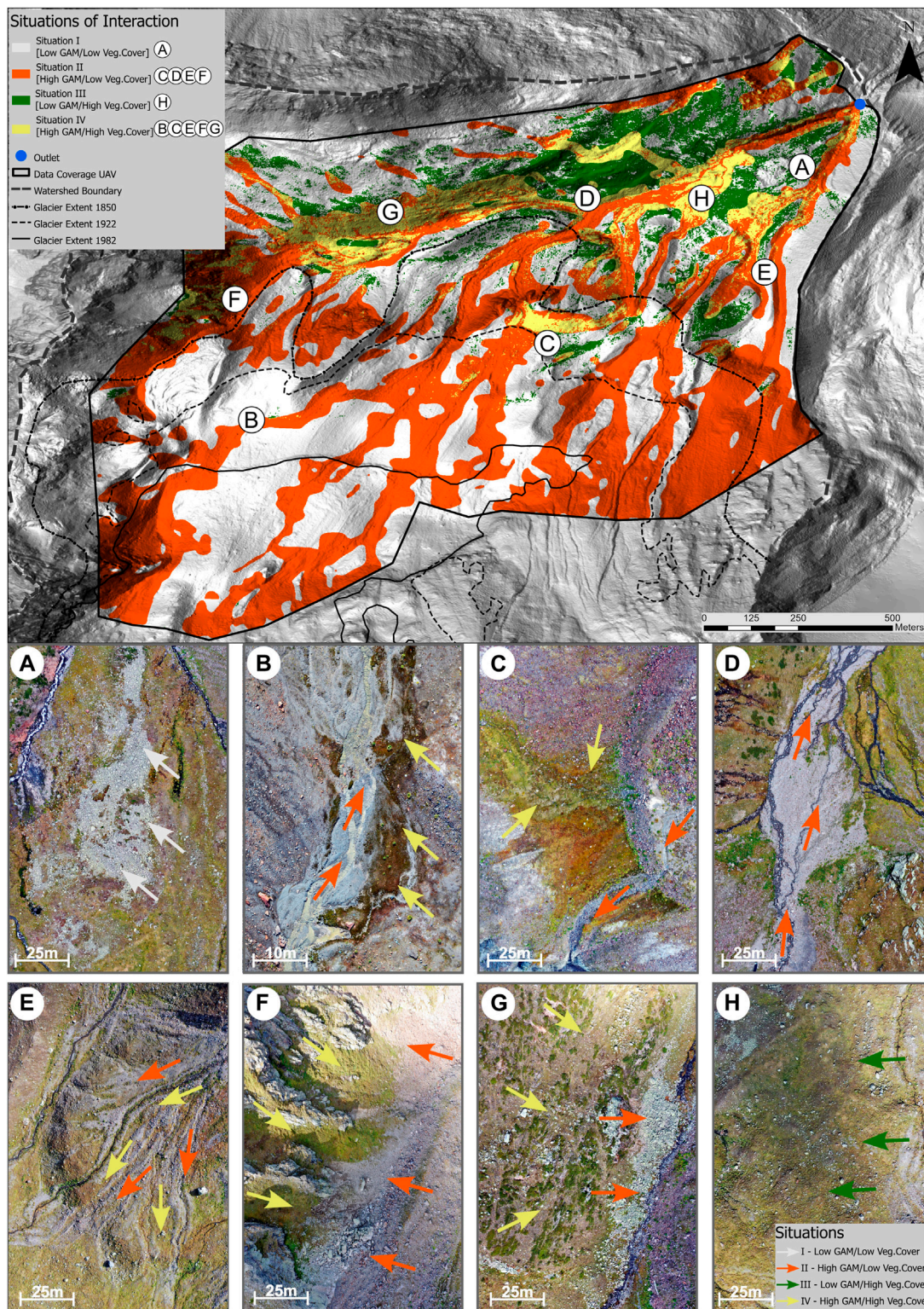


**FIGURE 8**

The four situations of the Interaction between GAM and Vegetation distribution with Example Pictures. (A) Illustrates high and low vegetation cover next to each other in an area with high terrain age and low GAM. (B) Shows the first dense vegetation patch in an area of fluvial deposition, approximately 50 years after glacier retreat. (C) Represents the largest vegetation patch that occurs between 100 and 170 years of glacier retreat in an area of former fluvial activity. (D) Depicts low vegetation cover in an area of fluvial accumulation outside the LIA margin. (E) Demonstrates a sequence of vegetated and unvegetated areas in the accumulation zone of debris flow activity, which is due to differences in the timing and magnitude of debris flow activity. (F) Displays steep, densely vegetated safe sites on slopes prone to rockfall, while the accumulation area of recent rockfall activity shows no vegetation. (G) Shows a steep south-facing slope outside the LIA moraine that is already inactive despite high GAM results, with only small bedrock outcrops and the rockfall accumulation area still showing vegetation cover. (H) Illustrates a flat, densely vegetated area outside the LIA moraine with low GAM results.

vegetation succession, enhancing our comprehension of their interplay.

## Conclusion

In this study, we presented a first attempt to investigate catchment-scale geomorphic activity and its association with vegetation distribution on drift-mantled slopes and the glaciofluvial plain in a proglacial environment.

Our multi-proxy analysis represents an important step towards understanding the catchment-wide influence of geomorphic processes on plant colonization. The results suggest that geomorphic activity acts as a second-order determinant for vegetation distribution, contributing to the resulting spatial heterogeneity of colonization.

Our mapping of cover thresholds highlighted the significance of geomorphic pulses on the glaciofluvial plain. These pulses facilitate initial vegetation colonization. However, high-magnitude geomorphic processes, especially fluvial and debris flow processes, have the potential to reset established vegetation. We identified areas where stability thresholds were met, which can be associated with potential ecosystem engineering during the biogeomorphic succession.

The observations highlighted the challenges of interpreting biogeomorphic succession along a terrain age gradient at the catchment scale in glacier forelands, given the complex biogeomorphic mosaic observed. The introduced time-independent framework, focusing on the relationship between geomorphic activity and the stabilizing effect of vegetation, provides a systematic approach to examining biogeomorphic succession across diverse situations.

The methods employed represent a trade-off between the level of detail and the scale of observation. There is potential to improve the precision of mapping geomorphic activity, and it is essential to extend the spectrum of processes studied, including rockfall events. Beyond vegetation cover, a comprehensive understanding of successional stages should factor in vegetation composition.

## Data availability statement

The original contributions presented in the study are included in the article/[Supplementary Material](#), further inquiries can be directed to the corresponding author.

## References

- Baewert, H., and Morche, D. (2014). Coarse sediment dynamics in a proglacial fluvial system (Fagge River, Tyrol). *Geomorphology* 218, 88–97. doi:10.1016/j.geomorph.2013.10.021
- Ballantyne, C. K. (2002). Paraglacial geomorphology. *Quat. Sci. Rev.* 21, 1935–2017. doi:10.1016/s0277-3791(02)00005-7
- Beven, K. J., and Kirkby, M. J. (1979). A physically based, variable contributing area model of basin hydrology/Un modèle à base physique de zone d'appel variable de l'hydrologie du bassin versant. *Hydrological Sci. J.* 24, 43–69. doi:10.1080/02626667909491834
- Bishop, T., and Mcbratney, A. (2001). A comparison of prediction methods for the creation of field-extent soil property maps. *Geoderma* 103, 149–160. doi:10.1016/s0016-7061(01)00074-x
- Bormann, F. H., and Likens, G. E. (2012). Pattern and process in a forested ecosystem: disturbance, development and the steady state based on the Hubbard Brook ecosystem study. *Springer Sci. Bus. Media*. doi:10.1126/science.205.4413.1369
- Bosson, J.-B., Huss, M., Cauvy-Fraunié, S., Clément, J.-C., Costes, G., Fischer, M., et al. (2023). Future emergence of new ecosystems caused by glacial retreat. *Nature* 620, 562–569. doi:10.1038/s41586-023-06302-2
- Braun, M. T., and Oswald, F. L. (2011). Exploratory regression analysis: a tool for selecting models and determining predictor importance. *Behav. Res. Methods* 43, 331–339. doi:10.3758/s13428-010-0046-8
- Burga, C. A., Krüsi, B., Egli, M., Wernli, M., Elsener, S., Ziefle, M., et al. (2010). Plant succession and soil development on the foreland of the Morteratsch glacier (Pontresina,

## Author contributions

SH: Conceptualization, Data curation, Formal Analysis, Investigation, Methodology, Validation, Visualization, Writing—original draft, Writing—review and editing. SS: Formal Analysis, Methodology, Software, Writing—review and editing. J-CO: Conceptualization, Methodology, Project administration, Resources, Supervision, Writing—review and editing. UZ: Data curation, Software, Writing—review and editing. L-MO: Data curation, Investigation, Writing—review and editing. RJ: Supervision, Writing—review and editing. SK: Conceptualization, Funding acquisition, Project administration, Resources, Supervision, Writing—review and editing.

## Funding

The author(s) declare financial support was received for the research, authorship, and/or publication of this article. This study was carried out as part of the PHUSICOS project, which is funded by the European Union's Horizon 2020 research and innovation programme under grant agreement No. 776681.

## Conflict of interest

The authors declare that the research was conducted in the absence of any commercial or financial relationships that could be construed as a potential conflict of interest.

## Publisher's note

All claims expressed in this article are solely those of the authors and do not necessarily represent those of their affiliated organizations, or those of the publisher, the editors and the reviewers. Any product that may be evaluated in this article, or claim that may be made by its manufacturer, is not guaranteed or endorsed by the publisher.

## Supplementary material

The Supplementary Material for this article can be found online at: <https://www.frontiersin.org/articles/10.3389/feart.2023.1280375/full#supplementary-material>

- Switzerland): straight forward or chaotic? *Flora - Morphol. Distribution, Funct. Ecol. Plants* 205, 561–576. doi:10.1016/j.flora.2009.10.001
- Caccianiga, M., Luzzaro, A., Pierce, S., Ceriani, R. M., and Cerabolini, B. (2006). The functional basis of a primary succession resolved by CSR classification. *Oikos* 112, 10–20. doi:10.1111/j.0030-1299.2006.14107.x
- Carrivick, J. L., and Heckmann, T. (2017). Short-term geomorphological evolution of proglacial systems. *Geomorphology* 287, 3–28. doi:10.1016/j.geomorph.2017.01.037
- Cavalli, M., Trevisani, S., Comiti, F., and Marchi, L. (2013). Geomorphometric assessment of spatial sediment connectivity in small Alpine catchments. *Geomorphology* 188, 31–41. doi:10.1016/j.geomorph.2012.05.007
- Chandler, B. M. P., Lovell, H., Boston, C. M., Lukas, S., Barr, I. D., Benediktsson, Í. Ö., et al. (2018). Glacial geomorphological mapping: a review of approaches and frameworks for best practice. *Earth-Science Rev.* 185, 806–846. doi:10.1016/j.earscirev.2018.07.015
- Chapin, F. S., Walker, L. R., Fastie, C. L., and Sharman, L. C. (1994). Mechanisms of primary succession following deglaciation at Glacier Bay, Alaska. *Ecol. Monogr.* 64, 149–175. doi:10.2307/2937039
- Cienciala, P., Nelson, A. D., Haas, A. D., and Xu, Z. (2020). Lateral geomorphic connectivity in a fluvial landscape system: unraveling the role of confinement, biogeomorphic interactions, and glacial legacies. *Geomorphology* 354, 107036. doi:10.1016/j.geomorph.2020.107036
- Connell, J. H. (1978). Diversity in tropical rain forests and coral reefs: high diversity of trees and corals is maintained only in a nonequilibrium state. *Science* 199, 1302–1310. doi:10.1126/science.199.4335.1302
- Conrad, O., Bechtel, B., Bock, M., Dietrich, H., Fischer, E., Gerlitz, L., et al. (2015). System for automated geoscientific analyses (SAGA) v. 2.1. 4. *Geosci. Model Dev.* 8, 1991–2007. doi:10.5194/gmd-8-1991-2015
- Corenblit, D., Steiger, J., Gurnell, A. M., Tabacchi, E., and Roques, L. (2009). Control of sediment dynamics by vegetation as a key function driving biogeomorphic succession within fluvial corridors. *Earth Surf. Process. Landforms* 34, 1790–1810. doi:10.1002/esp.1876
- Cox, N. J. (2007). Kernel estimation as a basic tool for geomorphological data analysis. *Earth Surf. Process. Landforms* 32, 1902–1912. doi:10.1002/esp.1518
- Curry, A. M., Cleasby, V., and Zukowskyj, P. (2006). Paraglacial response of steep, sediment-mantled slopes to post-Little Ice Age glacier recession in the central Swiss Alps. *J. Quat. Sci.* 21, 211–225. doi:10.1002/jqs.954
- Cutler, N. A., Belyea, L. R., and Dugmore, A. J. (2008b). The spatiotemporal dynamics of a primary succession. *J. Ecol.* 96, 231–246. doi:10.1111/j.1365-2745.2007.01344.x
- Cutler, N., Belyea, L., and Dugmore, A. (2008a). The spatiotemporal dynamics of a primary succession. *J. Ecol.* 96, 231–246. doi:10.1111/j.1365-2745.2007.01344.x
- Cutler, N. (2010). Long-term primary succession: a comparison of non-spatial and spatially explicit inferential techniques. *Plant Ecol.* 208, 123–136. doi:10.1007/s11258-009-9692-2
- D'Amico, M. E., Freppaz, M., Filipa, G., and Zanini, E. (2014). Vegetation influence on soil formation rate in a proglacial chronosequence (Lys Glacier, NW Italian Alps). *Catena* 113, 122–137. doi:10.1016/j.catena.2013.10.001
- DE Haas, T., Densmore, A., Stoffel, M., Suwa, H., Imaizumi, F., Ballesteros-Cánovas, J., et al. (2018). Avulsions and the spatio-temporal evolution of debris-flow fans. *Earth-Science Rev.* 177, 53–75. doi:10.1016/j.earscirev.2017.11.007
- Dietrich, W. E., and Perron, J. T. (2006). The search for a topographic signature of life. *Nature* 439, 411–418. doi:10.1038/nature04452
- Dühnforth, M., Densmore, A. L., Ivy-Ochs, S., Allen, P. A., and Kubik, P. W. (2007). Timing and patterns of debris flow deposition on Shepherd and Symmes creek fans, Owens Valley, California, deduced from cosmogenic <sup>10</sup>Be. *J. Geophys. Res. Earth Surf.* 112, F03S15. doi:10.1029/2006jfe000562
- Dusik, J.-M., Leopold, M., and Haas, F. (2019a). Periglacial morphodynamics in the upper Kaunertal. *Geomorphol. Proglacial Syst.* doi:10.1007/978-3-319-94184-4\_7
- Dusik, J.-M., Neugirg, F., and Haas, F. (2019b). Slope wash, gully erosion and debris flows on lateral moraines in the upper Kaunertal, Austria. *Geomorphol. Proglacial Syst.* doi:10.1007/978-3-319-94184-4\_11
- Eichel, J., Corenblit, D., and Dikau, R. (2016). Conditions for feedbacks between geomorphic and vegetation dynamics on lateral moraine slopes: a biogeomorphic feedback window. *Earth Surf. Process. Landforms* 41, 406–419. doi:10.1002/esp.3859
- Eichel, J., Draebing, D., Klingbeil, L., Wieland, M., Eling, C., Schmidlein, S., et al. (2017). Solifluction meets vegetation: the role of biogeomorphic feedbacks for turf-banked solifluction lobe development. *Earth Surf. Process. Landforms* 42, 1623–1635. doi:10.1002/esp.4102
- Eichel, J., Draebing, D., and Meyer, N. (2018). From active to stable: paraglacial transition of Alpine lateral moraine slopes. *Land Degrad. Dev.* 29, 4158–4172. doi:10.1002/ldr.3140
- Eichel, J., Draebing, D., Winkler, S., and Meyer, N. (2023). Similar vegetation-geomorphic disturbance feedbacks shape unstable glacier forelands across mountain regions. *Ecosphere* 14, e4404. doi:10.1002/ecs2.4404
- Eichel, J., Krautblatter, M., Schmidlein, S., and Dikau, R. (2013). Biogeomorphic interactions in the Turtmann glacier forefield, Switzerland. *Geomorphology* 201, 98–110. doi:10.1016/j.geomorph.2013.06.012
- Erschbamer, B., and Caccianiga, M. S. (2017). Glacier forelands: lessons of plant population and community development. *Prog. Bot.* 78, 259–284. doi:10.1007/124\_2016\_4
- Fastie, C. L. (1995). Causes and ecosystem consequences of multiple pathways of primary succession at Glacier Bay, Alaska. *Ecology* 76, 1899–1916. doi:10.2307/1940722
- Ferrer-Boix, C., Chartrand, S. M., Hassan, M. A., Martín-Vide, J. P., and Parker, G. (2016). On how spatial variations of channel width influence river profile curvature. *Geophys. Res. Lett.* 43, 6313–6323. doi:10.1002/2016gl069824
- Fickert, T. (2017). *Glaciers evolution in a changing world*. Glacier forelands – unique field laboratories for the study of primary succession of plants
- Fischer, A., Fickert, T., Schwaizer, G., Patzelt, G., and Gross, G. (2019). Vegetation dynamics in Alpine glacier forelands tackled from space. *Sci. Rep.* 9, 13918. doi:10.1038/s41598-019-50273-2
- Fliri, F. (1975). *Klima der Alpen im Raume von Tirol*. Univ. Verl. Wagner.
- Fryirs, K. A., Brierley, G. J., Preston, N. J., and Spencer, J. (2007b). Catchment-scale (dis)connectivity in sediment flux in the upper Hunter catchment, New South Wales, Australia. *Geomorphology* 84, 297–316. doi:10.1016/j.geomorph.2006.01.044
- Fryirs, K. A., Brierley, G. J., Preston, N. J., and Kasai, M. (2007a). Buffers, barriers and blankets: the (dis)connectivity of catchment-scale sediment cascades. *Catena* 70, 49–67. doi:10.1016/j.catena.2006.07.007
- Geilhausen, M., Morche, D., Otto, J.-C., and Schrott, L. (2013). Sediment discharge from the proglacial zone of a retreating Alpine glacier. *Z. für Geomorphol. Suppl. Issues* 57, 29–53. doi:10.1127/0372-8854/2012/s-00122
- Geilhausen, M., Otto, J.-C., and Schrott, L. (2012). Spatial distribution of sediment storage types in two glacier landsystems (Pasterze and Obersulzbachkees, Hohe Tauern, Austria). *J. Maps* 8, 242–259. doi:10.1080/17445647.2012.708540
- Gentili, R., Armiraglio, S., Rossi, G., Sgorbati, S., and Baroni, C. (2010). Floristic patterns, ecological gradients and biodiversity in the composite channels (Central Alps, Italy). *Flora-Morphology, Distribution, Funct. Ecol. Plants* 205, 388–398. doi:10.1016/j.flora.2009.12.013
- Graf, F., Frei, M., and Böll, A. (2009). Effects of vegetation on the angle of internal friction of a moraine. *For. Snow Landsc. Res.* 82, 61–77.
- Gurnell, A. M., Bertoldi, W., and Corenblit, D. (2012). Changing river channels: the roles of hydrological processes, plants and pioneer fluvial landforms in humid temperate, mixed load, gravel bed rivers. *Earth-Science Rev.* 111, 129–141. doi:10.1016/j.earscirev.2011.11.005
- Gurnell, A. M., Edwards, P. J., Petts, G. E., and Ward, J. V. (2000). A conceptual model for alpine proglacial river channel evolution under changing climatic conditions. *Catena* 38, 223–242. doi:10.1016/s0341-8162(99)00069-7
- Haas, F., Heckmann, T., Hilger, L., and Becht, M. (2012). Quantification and modelling of debris flows in the proglacial area of the Gepatschferner/Austria using ground-based LiDAR.
- Hammer, W. (1923). Erläuterungen zur geologische Spezialkarte der Republik Österreich: 1: 75.000. *Geol. Bundesanst. Blatt Nauders*.
- Hartl, L., and Fischer, A. (2014). The Gepatschferner from 1850 - 2006, with links to digital elevation models and glacier margins. *Suppl. Hartl. Lea* (2010): The Gepatschferner from 1850 - 2006 - Changes in length, area and volume in relation to climate. Diploma Thesis, Institute for Meteorology and Geophysics, University of Innsbruck, 79 pp, hdl:10013/epic.44273.d001. PANGAEA. doi:10.1594/PANGAEA.836949
- Haselberger, S., Ohler, L. M., Junker, R. R., Otto, J. C., Glade, T., and Kraushaar, S. (2021). Quantification of biogeomorphic interactions between small-scale sediment transport and primary vegetation succession on proglacial slopes of the Gepatschferner, Austria. *Earth Surf. Process. Landforms* 46, 1941–1952. doi:10.1002/esp.5136
- Heckmann, T., Hilger, L., Vehling, L., and Becht, M. (2016a). Integrating field measurements, a geomorphological map and stochastic modelling to estimate the spatially distributed rockfall sediment budget of the Upper Kaunertal, Austrian Central Alps. *Geomorphology* 260, 16–31. doi:10.1016/j.geomorph.2015.07.003
- Heckmann, T., Mccoll, S., and Morche, D. (2016b). Retreating ice: research in proglacial areas matters. *Earth Surf. Process. Landforms* 41, 271–276. doi:10.1002/esp.3858
- Heckmann, T., Morche, D., and Becht, M. (2019). *Geomorphology of proglacial systems*. Introduction
- Heckmann, T., and Vericat, D. (2018). Computing spatially distributed sediment delivery ratios: inferring functional sediment connectivity from repeat high-resolution digital elevation models. *Earth Surf. Process. Landforms* 43, 1547–1554. doi:10.1002/esp.4334
- Hilger, L., Dusik, J.-M., Heckmann, T., Haas, F., Glira, P., Pfeifer, N., et al. (2019). A sediment budget of the upper Kaunertal. *Geomorphol. Proglacial Syst.* doi:10.1007/978-3-319-94184-4\_17

- Hodgkins, R., Cooper, R., Wadham, J., and Tranter, M. (2003). Suspended sediment fluxes in a high-Arctic glacierised catchment: implications for fluvial sediment storage. *Sediment. Geol.* 162, 105–117. doi:10.1016/s0037-0738(03)00218-5
- Huston, M. A., and Huston, M. A. (1994). *Biological diversity: the coexistence of species*. Cambridge University Press.
- Isselin-Nondedeu, F., and Bédécarrats, A. (2007). Influence of alpine plants growing on steep slopes on sediment trapping and transport by runoff. *Catena* 71, 330–339. doi:10.1016/j.catena.2007.02.001
- James, L. A., Hodgson, M. E., Ghoshal, S., and Latiolais, M. M. (2012). Geomorphic change detection using historic maps and DEM differencing: the temporal dimension of geospatial analysis. *Geomorphology* 137, 181–198. doi:10.1016/j.geomorph.2010.10.039
- James, M. R., and Robson, S. (2012). Straightforward reconstruction of 3D surfaces and topography with a camera: accuracy and geoscience application. *J. Geophys. Res. Earth Surf.* 117. doi:10.1029/2011jf002289
- Jumpponen, A., Väre, H., Mattson, K. G., Ohtonen, R., and Trappe, J. M. (1999). Characterization of 'safe sites' for pioneers in primary succession on recently deglaciated terrain. *J. Ecol.* 87, 98–105. doi:10.1046/j.1365-2745.1999.00328.x
- Junker, R. R., Hanusch, M., He, X., Ruiz-Hernández, V., Otto, J.-C., Kraushaar, S., et al. (2020). Ödenwinkel: an Alpine platform for observational and experimental research on the emergence of multidiversity and ecosystem complexity. *Web Ecol.* 20, 95–106. doi:10.5194/we-20-95-2020
- Kassambara, A., and Kassambara, M. A. (2020). *Package 'ggpubr'*.
- Kellerer-Pirklbauer, G. K. L. A. A. (2019). Sammelbericht über die Gletschermessungen des Österreichischen Alpenvereins im Jahre 2018. *Bergauf*, 20–29.
- Kemppinen, J., Niittynen, P., Le Roux, P. C., Momberg, M., Happonen, K., Aalto, J., et al. (2021). Consistent trait–environment relationships within and across tundra plant communities. *Nat. Ecol. Evol.* 5, 458–467. doi:10.1038/s41559-021-01396-1
- Klaar, M. J., Kidd, C., Malone, E., Bartlett, R., Pinay, G., Chapin, F. S., et al. (2015). Vegetation succession in deglaciated landscapes: implications for sediment and landscape stability. *Earth Surf. Process. Landforms* 40, 1088–1100. doi:10.1002/esp.3691
- Körner, C. (2003). Alpine plant life: functional plant ecology of high mountain ecosystems; with 47 tables. *Springer Sci. Bus. Media*. doi:10.1007/978-3-642-18970-8
- Krivoruchko, K., and Gribov, A. (2019). Evaluation of empirical Bayesian kriging. *Spat. Stat.* 32, 100368. doi:10.1016/j.spa.2019.100368
- Krivoruchko, K. (2012). Modeling contamination using EmpiricalBayesian kriging. *ArcUser Fall*.
- Lane, S. N., Borgeaud, L., and Vittoz, P. (2016). Emergent geomorphic–vegetation interactions on a subalpine alluvial fan. *Earth Surf. Process. Landforms* 41, 72–86. doi:10.1002/esp.3833
- Lane, S. N., Westaway, R. M., and Murray Hicks, D. (2003). Estimation of erosion and deposition volumes in a large, gravel-bed, braided river using synoptic remote sensing. *Earth Surf. Process. Landforms* 28, 249–271. doi:10.1002/esp.483
- Larsen, A., Nardin, W., Lageweg, W. I., and Bätz, N. (2020). Biogeomorphology, *quo vadis?* On processes, time, and space in biogeomorphology. *Earth Surf. Process. Landforms* 46, 12–23. doi:10.1002/esp.5016
- Marston, R. A. (2010). Geomorphology and vegetation on hillslopes: interactions, dependencies, and feedback loops. *Geomorphology* 116, 206–217. doi:10.1016/j.geomorph.2009.09.028
- Marteinsdóttir, B., Svavarsdóttir, K., and Þórhallsdóttir, T. E. (2010). Development of vegetation patterns in early primary succession. *J. Veg. Sci.* 21, 531–540. doi:10.1111/j.1654-1103.2009.01161.x
- Martin, C., Pohl, M., Alewell, C., Körner, C., and Rixen, C. (2010). Interrill erosion at disturbed alpine sites: effects of plant functional diversity and vegetation cover. *Basic Appl. Ecol.* 11, 619–626. doi:10.1016/j.baae.2010.04.006
- Matthews, J. A. (1999). Disturbance regimes and ecosystem response on recently-deglaciated substrates. *Ecosyst. World*, 17–38.
- Matthews, J. A. (1992). *The ecology of recently-deglaciated terrain: a geoecological approach to glacier forelands*. Cambridge University Press.
- Matthews, J. A., and Vater, A. E. (2015). Pioneer zone geo-ecological change: observations from a chronosequence on the Storbreen glacier foreland, Jotunheimen, southern Norway. *Catena* 135, 219–230. doi:10.1016/j.catena.2015.07.016
- Meusburger, K., Konz, N., Schaub, M., and Alewell, C. (2010). Soil erosion modelled with USLE and PESERA using QuickBird derived vegetation parameters in an alpine catchment. *Int. J. Appl. Earth Observation Geoinformation* 12, 208–215. doi:10.1016/j.jag.2010.02.004
- Miller, H. R., and Lane, S. N. (2018). Biogeomorphic feedbacks and the ecosystem engineering of recently deglaciated terrain. *Prog. Phys. Geogr. Earth Environ.* 43, 24–45. doi:10.1177/0309133318816536
- Moore, I., Burch, G., and Mackenzie, D. (1988). Topographic effects on the distribution of surface soil water and the location of ephemeral gullies. *Trans. ASAE* 31, 1098–1107. doi:10.13031/2013.30829
- Moore, I. D., Grayson, R., and Ladson, A. (1991). Digital terrain modelling: a review of hydrological, geomorphological, and biological applications. *Hydrol. Process.* 5, 3–30. doi:10.1002/hyp.3360050103
- Morche, D., Baewert, H., Schuchardt, A., Faust, M., Weber, M., and Khan, T. (2019). Fluvial sediment transport in the proglacial fagge river, Kaunertal, Austria. *Geomorphol. Proglacial Syst.* doi:10.1007/978-3-319-94184-4\_13
- Moreau, M., Mercier, D., Laffly, D., and Roussel, E. (2008). Impacts of recent paraglacial dynamics on plant colonization: a case study on Midtre Lovénbreen foreland, Spitsbergen (79°N). *Geomorphology* 95, 48–60. doi:10.1016/j.geomorph.2006.07.031
- Nicoll, T., and Brierley, G. (2017). Within-catchment variability in landscape connectivity measures in the Garang catchment, upper Yellow River. *Geomorphology* 277, 197–209. doi:10.1016/j.geomorph.2016.03.014
- Ohler, L.-M., Haselberger, S., Janssen, S., Otto, J.-C., Kraushaar, S., and Junker, R. R. (2023). Proglacial slopes are protected against erosion by trait diverse and dense plant communities associated with specific microbial communities. *Basic Appl. Ecol.* 71, 57–71. doi:10.1016/j.baae.2023.05.008
- Otto, J.-C., Schrott, L., and Keller, F. (2020). *Map of permafrost distribution for Austria, Europe*. PANGAEA.
- Otto, J.-C., and Dikau, R. (2004). Geomorphologic system analysis of a high mountain valley in the Swiss Alps. *Z. für Geomorphol.* 48, 323–342. doi:10.1127/zfg/48/2004/323
- Otto, J.-C., Schrott, L., Jaboyedoff, M., and Dikau, R. (2009). Quantifying sediment storage in a high alpine valley (Turtmanntal, Switzerland). *Earth Surf. Process. Landforms* 34, 1726–1742. doi:10.1002/esp.1856
- Poesen, J., and Lavee, H. (1994). Rock fragments in top soils: significance and processes. *Catena* 23, 1–28. doi:10.1016/0341-8162(94)90050-7
- Porter, P. R., Smart, M. J., and Irvine-Fynn, T. D. L. (2019). Glacial sediment stores and their reworking. *Geomorphol. Proglacial Syst.* doi:10.1007/978-3-319-94184-4\_10
- Raffl, C., Mallaun, M., Mayer, R., and Erschbamer, B. (2006). Vegetation succession pattern and diversity changes in a glacier valley, Central Alps, Austria. *Arct. Antarct. Alp. Res.* 38, 421–428. doi:10.1657/1523-0430(2006)38[421:vspadc]2.0.co;2
- Reinhardt, L., Jerolmack, D., Cardinale, B. J., Vanacker, V., and Wright, J. (2010). Dynamic interactions of life and its landscape: feedbacks at the interface of geomorphology and ecology. *Earth Surf. Process. Landforms* 35, 78–101. doi:10.1002/esp.1912
- Renschler, C. S., Doyle, M. W., and Thoms, M. (2007). Geomorphology and ecosystems: challenges and keys for success in bridging disciplines. *Geomorphology* 89, 1–8. doi:10.1016/j.geomorph.2006.07.011
- Richards, K., Brasington, J., and Hughes, F. (2002). Geomorphic dynamics of floodplains: ecological implications and a potential modelling strategy. *Freshw. Biol.* 47, 559–579. doi:10.1046/j.1365-2427.2002.00920.x
- Robbins, J. A., and Matthews, J. A. (2018). Regional variation in successional trajectories and rates of vegetation change on glacier forelands in south-Central Norway. *Arct. Antarct. Alp. Res.* 42, 351–361. doi:10.1657/1938-4246-42.3.351
- Roncoroni, M., Brandani, J., Battin, T. I., and Lane, S. N. (2019). Ecosystem engineers: biofilms and the ontogeny of glacier floodplain ecosystems. *WIREs Water* 6. doi:10.1002/wat2.1390
- Sailer, R., Bollmann, E., Hoinkes, S., Rieg, L., Sproß, M., and Stötter, J. (2012). Quantification of geomorphodynamics in glaciated and recently deglaciated terrain based on airborne laser scanning data. *Geogr. Ann. Ser. A, Phys. Geogr.* 94, 17–32. doi:10.1111/j.1468-0459.2012.00456.x
- Schmidt, S., Ballabio, C., Alewell, C., Panagos, P., and Meusburger, K. (2018). Filling the European blank spot—Swiss soil erodibility assessment with topsoil samples. *J. Plant Nutr. Soil Sci.* 181, 737–748. doi:10.1002/jpln.201800128
- Schmidt, S., Porazinska, D., Conciencia, B.-L., Darcy, J., King, A., and Nemergut, D. (2016). Biogeochemical stoichiometry reveals P and N limitation across the post-glacial landscape of Denali National Park, Alaska. *Ecosystems* 19, 1164–1177. doi:10.1007/s10021-016-9992-z
- Schmidt, S., Tresch, S., and Meusburger, K. (2019). Modification of the RUSLE slope length and steepness factor (LS-factor) based on rainfall experiments at steep alpine grasslands. *MethodsX* 6, 219–229. doi:10.1016/j.mex.2019.01.004
- Sitzia, T., Picco, L., Ravazzolo, D., Comiti, F., Mao, L., and Lenzi, M. A. (2016). Relationships between woody vegetation and geomorphological patterns in three gravel-bed rivers with different intensities of anthropogenic disturbance. *Adv. Water Resour.* 93, 193–204. doi:10.1016/j.advwatres.2015.11.016
- Smith, M. J., Hillier, J., Otto, J.-C., and Geilhausen, M. (2013). *Geovisualization*.
- Stawska, M. (2017). Impacts of geomorphic disturbances on plant colonization in ebba valley, central spitsbergen, svalbard. *Quaest. Geogr.* 36, 51–64. doi:10.1515/quaest-2017-0004
- Stocker-Waldhuber, M., and Kuhn, M. (2019). Closing the balances of ice, water and sediment fluxes through the terminus of Gepatschferner. *Geomorphol. Proglacial Syst.* doi:10.1007/978-3-319-94184-4\_5
- Summerfield, M. A. (2005). A tale of two scales, or the two geomorphologies. *Trans. Inst. Br. Geogr.* 30, 402–415. doi:10.1111/j.1475-5661.2005.00182.x

- Temme, A. J. A. M., Heckmann, T., and Harlaar, P. (2016). Silent play in a loud theatre — dominantly time-dependent soil development in the geomorphically active proglacial area of the Gepatsch glacier, Austria. *Catena* 147, 40–50. doi:10.1016/j.catena.2016.06.042
- Thoms, M. C., Meitzen, K. M., Julian, J. P., and Butler, D. R. (2018). Biogeomorphology and resilience thinking: common ground and challenges. *Geomorphology* 305, 1–7. doi:10.1016/j.geomorph.2018.01.021
- Vehling, L., Rohn, J., and Moser, M. (2019). Rockfall at proglacial rockwalls—a case study from the Kaunertal, Austria. *Geomorphol. Proglacial Syst.* doi:10.1007/978-3-319-94184-4\_9
- Viles, H. A. (1988). *Biogeomorphology*, B. Blackwell.
- Viles, H. A., Naylor, L. A., Carter, N. E. A., and Chaput, D. (2008). Biogeomorphological disturbance regimes: progress in linking ecological and geomorphological systems. *Earth Surf. Process. Landforms* 33, 1419–1435. doi:10.1002/esp.1717
- Viles, H. (2020). Biogeomorphology: past, present and future. *Geomorphology* 366, 106809. doi:10.1016/j.geomorph.2019.06.022
- Wietrzyk, P., Rola, K., Osyczka, P., Nicia, P., Szymański, W., and Węgrzyn, M. (2018). The relationships between soil chemical properties and vegetation succession in the aspect of changes of distance from the glacier forehead and time elapsed after glacier retreat in the Irenebreen foreland (NW Svalbard). *Plant Soil* 428, 195–211. doi:10.1007/s11104-018-3660-3
- Wilcoxon, F. (1947). Probability tables for individual comparisons by ranking methods. *Biometrics* 3, 119–122. doi:10.2307/3001946
- Wojcik, R., Donhauser, J., Frey, B., and Benning, L. G. (2020). Time since deglaciation and geomorphological disturbances determine the patterns of geochemical, mineralogical and microbial successions in an Icelandic foreland. *Geoderma* 379, 114578. doi:10.1016/j.geoderma.2020.114578
- Wojcik, R., Eichel, J., Bradley, J. A., and Benning, L. G. (2021). How allogenic factors affect succession in glacier forefields. *Earth-Science Rev.* 218, 103642. doi:10.1016/j.earscirev.2021.103642
- Zangerl, U., Haselberger, S., and Kraushaar, S. (2022). Classifying sparse vegetation in a proglacial valley using UAV imagery and random forest algorithm. *Remote Sens.* 14, 4919. doi:10.3390/rs14194919